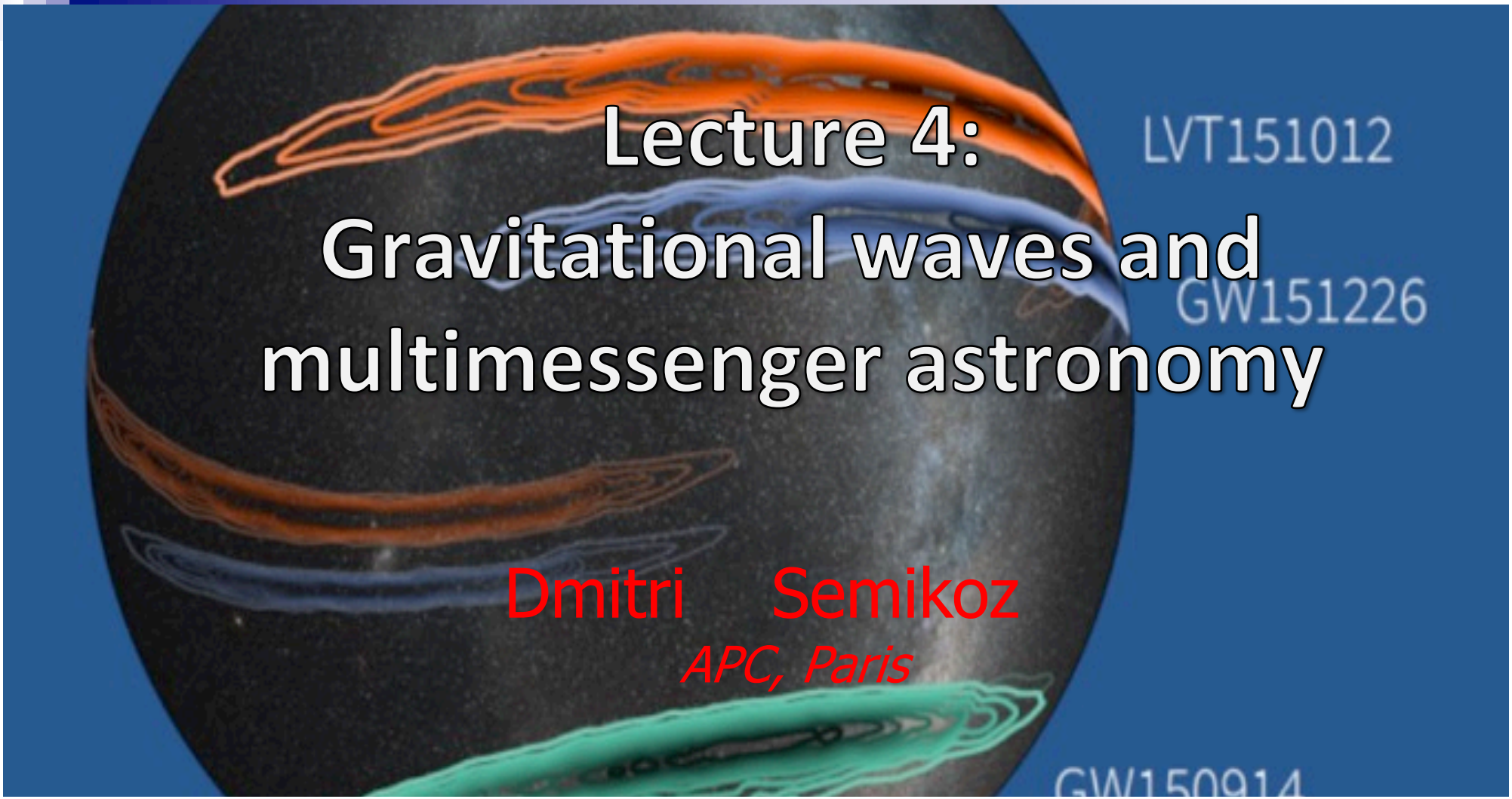

Lecture 4: Gravitational waves and multimessenger astronomy

Dmitri Semikoz
APC, Paris

Overview:

- *Introduction: history GW*
- *Ground based Experiments on Gravitational waves and first detection*
- *Phenomenology of Gravitational Waves*
- *LISA space mission*
- *Pulsar timing Arrays,*
- *HO measurement, NANOGrav signal*
- *Gravitational Waves from neutron star merge and multi-messenger signal.*

INTRODUCTION: histrory of Gravitational Wave searches

General Relativity

1915: Einstein's Theory of General Relativity

1916: Einstein paper on linear approximation to general relativity with multiple applications, including gravitational waves.

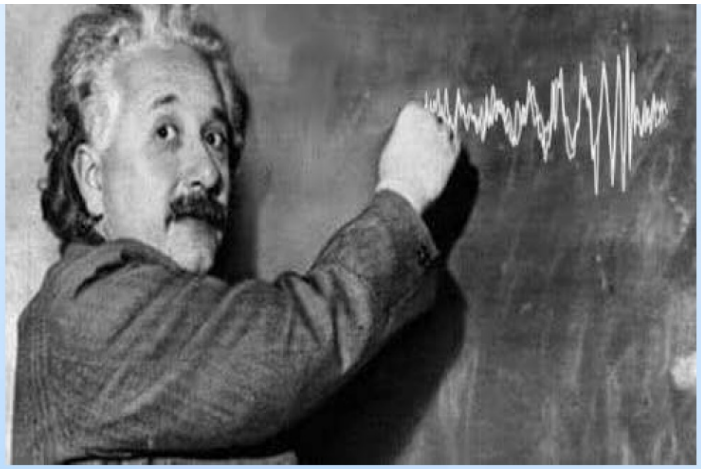

688 Sitzung der physikalisch-mathematischen Klasse vom 22. Juni 1916

Näherungsweise Integration der Feldgleichungen der Gravitation.

Von A. Einstein.

Gravitational waves

$$A = \frac{\varkappa}{24\pi} \sum_{\alpha\beta} \left(\frac{\partial^3 J_{\alpha\beta}}{\partial t^3} \right)^2 . \qquad (21)$$

Würde man die Zeit in Sekunden, die Energie in Erg messen, so würde zu diesem Ausdruck der Zahlenfaktor $\frac{1}{c^4}$ hinzutreten. Berücksichtigt man außerdem, daß $\varkappa = 1.87 \cdot 10^{-27}$, so sieht man, daß A in allen nur denkbaren Fällen einen praktisch verschwindenden Wert haben muß.

"… in all conceivable cases, ***A*** must have a practically vanishing value."

Gravitational waves are predicted by Einstein, but he recognizes that they are too small.

Gravitational waves

154 Gesamtsitzung vom 14. Februar 1918. — Mitteilung vom 31. Januar

Über Gravitationswellen.

Von A. Einstein.

On Gravitational Waves – 1918

Einstein works out the remaining details on gravitational waves: emission (quadrupole), polarizations, they carry energy, etc

Dabei ist zur Abkürzung

$$\mathfrak{J}_{\mu\nu} = \int x_\mu x_\nu \rho \, dV_0 \qquad (23)$$

gesetzt; $\mathfrak{J}_{\mu\nu}$ sind die Komponenten des (zeitlich variabeln) Trägheitsmomentes des materiellen Systems.

$$\gamma'_{23} = -\frac{\varkappa}{4\pi R}\ddot{\mathfrak{J}}_{23}.$$

Are Gravitational Waves Real?

Continued debate on whether gravitational waves really exist up until 1957 Chapel Hill conference.

Felix Pirani paper and presentation: relative acceleration of particle pairs can be associated with the Riemann tensor. The interpretation of the attendees was that non-zero components of the Riemann tensor were due to gravitational waves.

Sticky bead (Felix Pirani, Richard Feynman, Hermann Bondi)

Joe Weber of the University of Maryland, and from this inspiration started to think about gravitational wave detection.

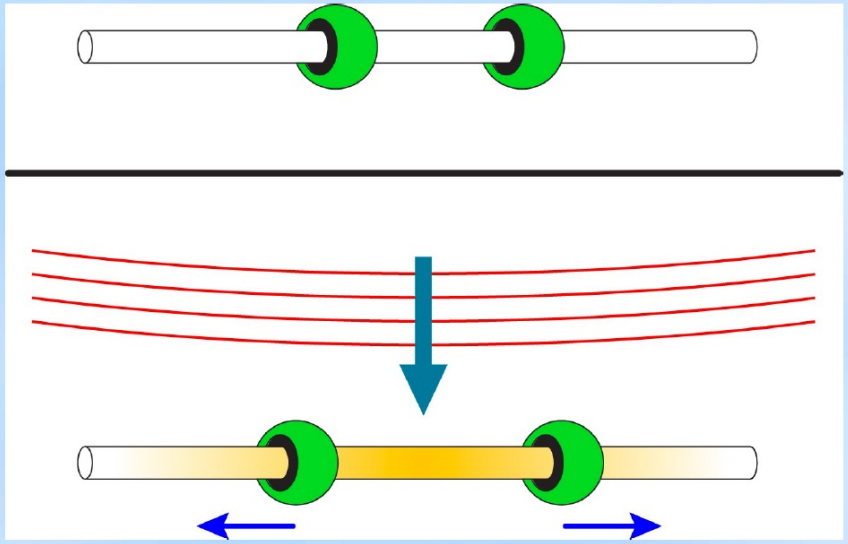

What Are Gravitational Waves?

- General relativity (1916) prediction.
- Gravity is not really a force in GR, but a space-time deformation.
- Masses locally deform space-time.
- Accelerated masses emit gravitational waves, ripples in space time.
- Space-time is rigid:

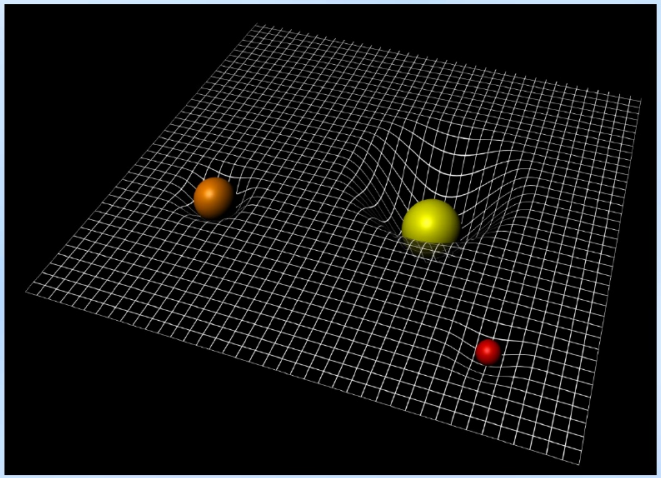

The amplitude of the deformation is tiny.

Need cataclysmic events in order to expect to measure something on Earth … $h \sim 10^{-21}$

- Gravitational Wave sources: mainly astrophysical in the 10 Hz -10 kHz bandwidth

Binary Pulsar PSR 1913+16

M1 = 1.438 M_o

M2 = 1.390 M_o

8 hour orbit

Orbit decays by 3mm per orbit.

Discovered in 1974 by Russell Hulse and Joseph Taylor, then at University Massachusetts.

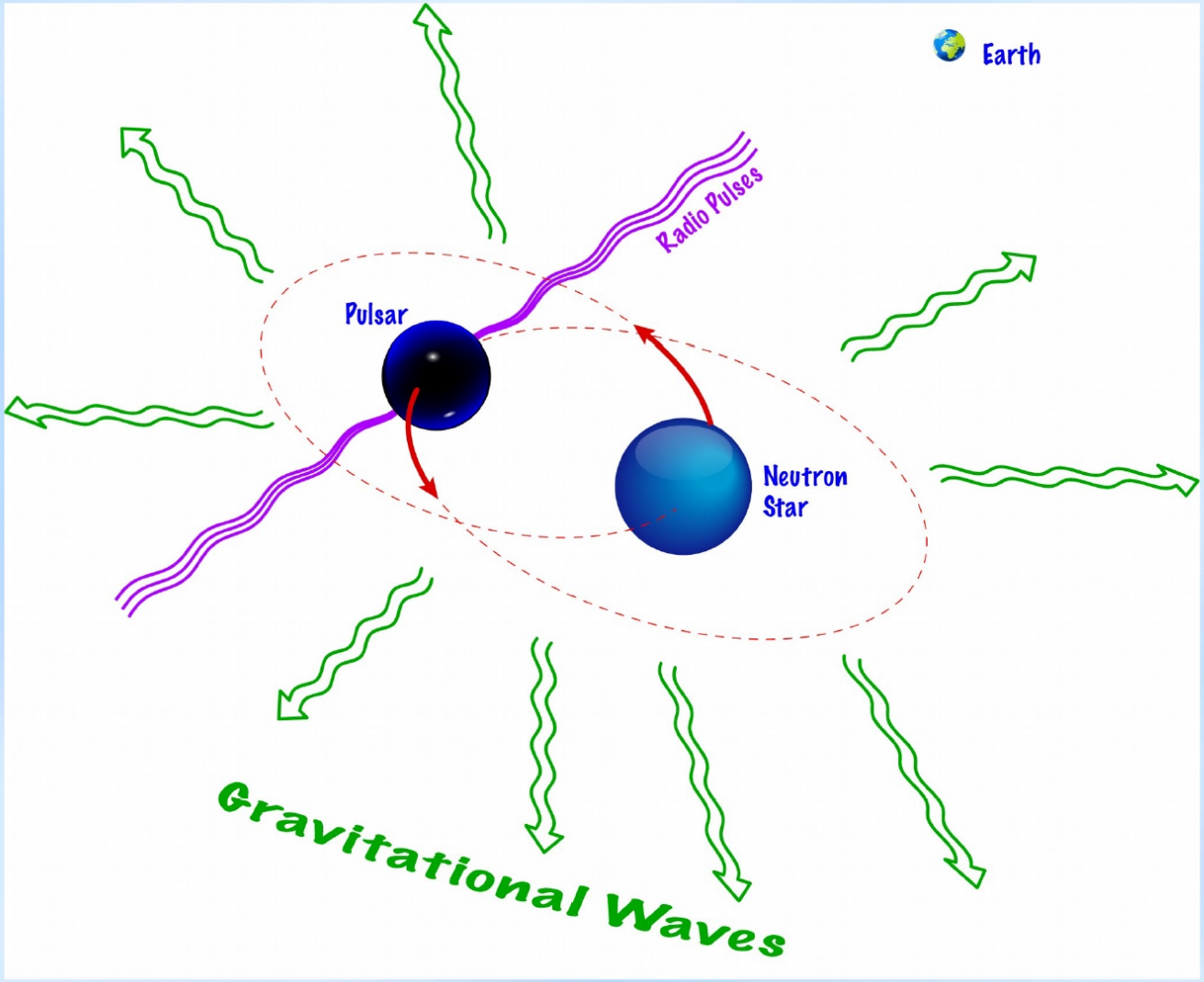

A Nobel Prize for ...

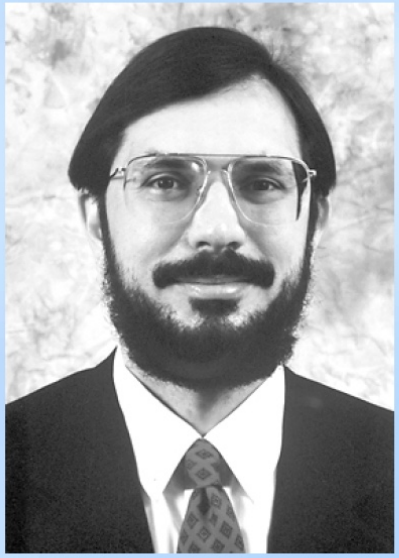

"… for the discovery of a new type of pulsar, a discovery that has opened up new possibilities for the study of gravitation." 1993

For more on this Nobel, see, "The Nobel pulsar", Nelson Christensen. Science, Vol. 348 no. 6236 p. 766 (2015).

First Proof That Gravitational Waves Exist - 1982

THE ASTROPHYSICAL JOURNAL, 253:908–920, 1982 February 15

A NEW TEST OF GENERAL RELATIVITY: GRAVITATIONAL RADIATION AND THE BINARY PULSAR PSR 1913+16

J. H. TAYLOR AND J. M. WEISBERG
Department of Physics and Astronomy, University of Massachusetts, Amherst; and Joseph Henry Laboratories, Physics Department, Princeton University
Received 1981 July 2; accepted 1981 August 28

ABSTRACT

Observations of pulse arrival times from the binary pulsar PSR 1913+16 between 1974 September and 1981 March are now sufficient to yield a solution for the component masses and the absolute size of the orbit. We find the total mass to be almost equally distributed between the pulsar and its unseen companion, with $m_p = 1.42 \pm 0.06\ M_\odot$ and $m_c = 1.41 \pm 0.06\ M_\odot$. These values are used, together with the well determined orbital period and eccentricity, to calculate the rate at which the orbital period should decay as energy is lost from the system via gravitational radiation. According to the general relativistic quadrupole formula, one should expect for the PSR 1913+16 system an orbital period derivative $\dot{P}_b = (-2.403 \pm 0.005) \times 10^{-12}$. Our observations yield the measured value $\dot{P}_b = (-2.30 \pm 0.22) \times 10^{-12}$. The excellent agreement provides compelling evidence for the existence of gravitational radiation, as well as a new and profound confirmation of the general theory of relativity.

Subject headings: gravitation — pulsars — relativity

Gravitational Wave Proof

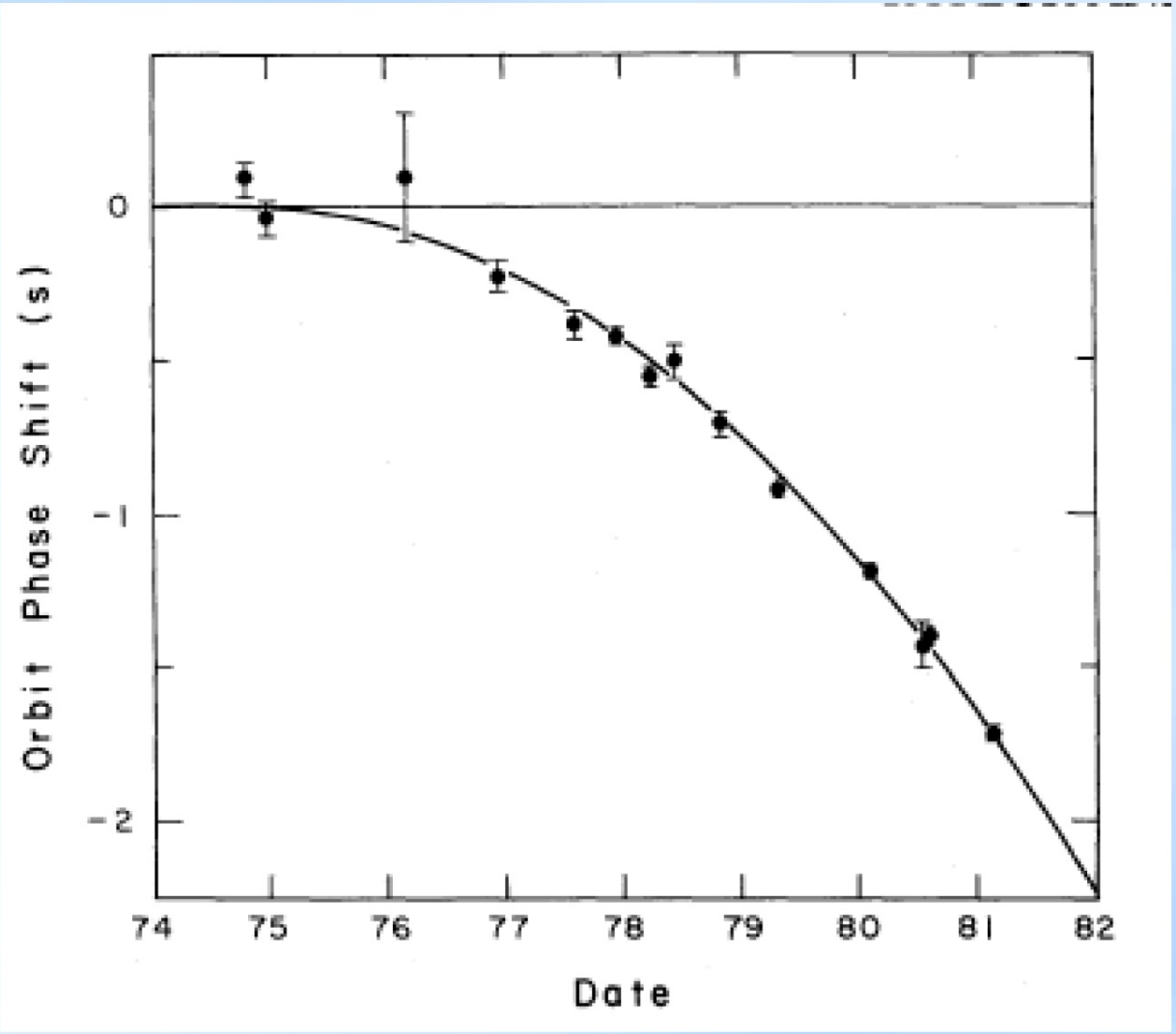

Taylor and Weisberg, 1982

Binary Pulsar Studies Continue

The Astrophysical Journal, 829:55 (10pp), 2016 September 20 doi:10.3847/0004-637X/829/1/55

RELATIVISTIC MEASUREMENTS FROM TIMING THE BINARY PULSAR PSR B1913+16

J. M. Weisberg and Y. Huang
Department of Physics and Astronomy, Carleton College, Northfield, MN 55057, USA; jweisber@carleton.edu
Received 2016 January 19; revised 2016 April 20; accepted 2016 June 1; published 2016 September 21

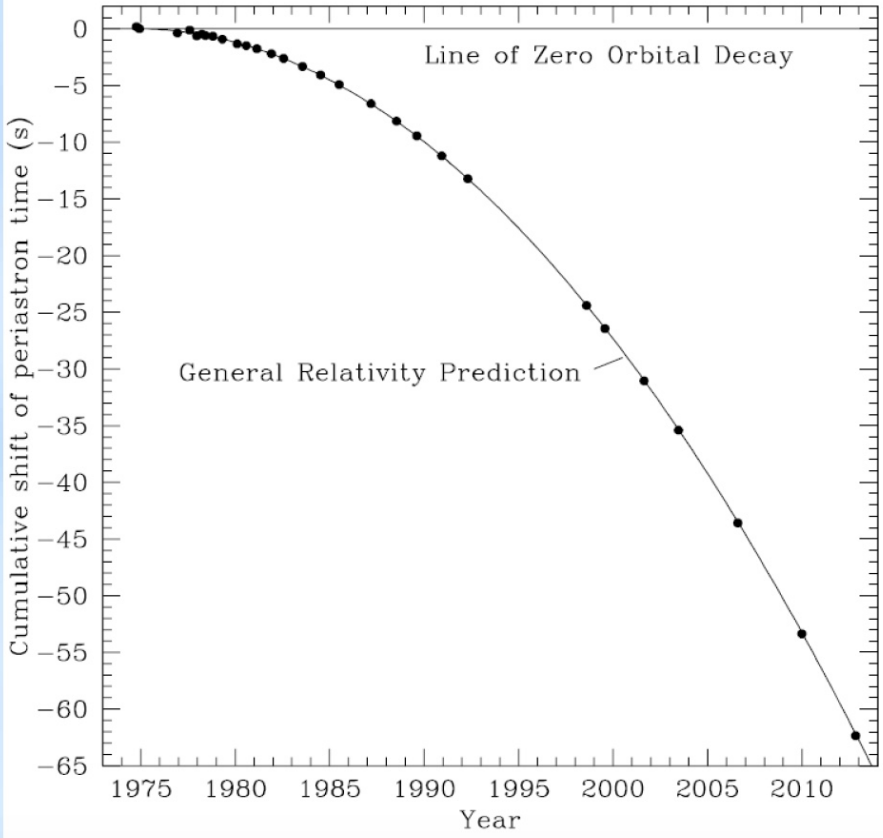

"The points, with error bars too small to show, represent our measurements"

Gravitational Wave Detection

Inspired and motivated by the Chapel Hill Conference, Joe Weber of the University of Maryland constructs the first gravitational wave detectors.

"In 1958 I was able to prove, using Einstein's equations that a gravitational wave would change the dimensions of an extended body."

EVIDENCE FOR DISCOVERY OF GRAVITATIONAL RADIATION*

J. Weber
Department of Physics and Astronomy, University of Maryland, College Park, Maryland 20742
(Received 29 April 1969)

Coincidences have been observed on gravitational-radiation detectors over a base line of about 1000 km at Argonne National Laboratory and at the University of Maryland. The probability that all of these coincidences were accidental is incredibly small. Experiments imply that electromagnetic and seismic effects can be ruled out with a high level of confidence. These data are consistent with the conclusion that the detectors are being excited by gravitational radiation.

K. Thorne 1980

1960s & 70s: Detection claims and theoretical studies on sources

The future looks promising—but by no means certain! The search for gravitational waves is a game requiring long, hard effort with a definite risk of total failure—but with very great payoff if it succeeds.

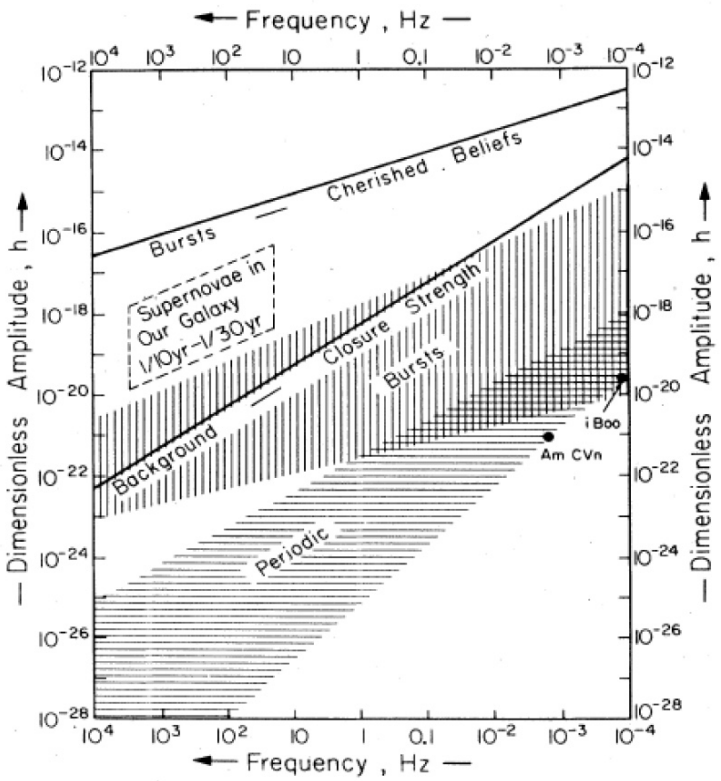

FIG. 3. Estimates of the strengths of the gravitational waves that bathe the Earth. See text for explanation of the lines and hatched regions.

Interferometric GW Detectors

First suggestion: 1962 two Soviet physicists, V.I. Pustovoit and M.E. Gertsenshtein, noted that the use of a Michelson interferometer would be a possible means to detect gravitational waves over a frequency range that was broader than the Weber bars.

1970's, Robert Forward (student of Weber) at Hughes Ai
Michelson interferometer to search for gravitational wave
(MIT) and astronaut Philip Chapman (also at MIT) for ins

The wideband interf

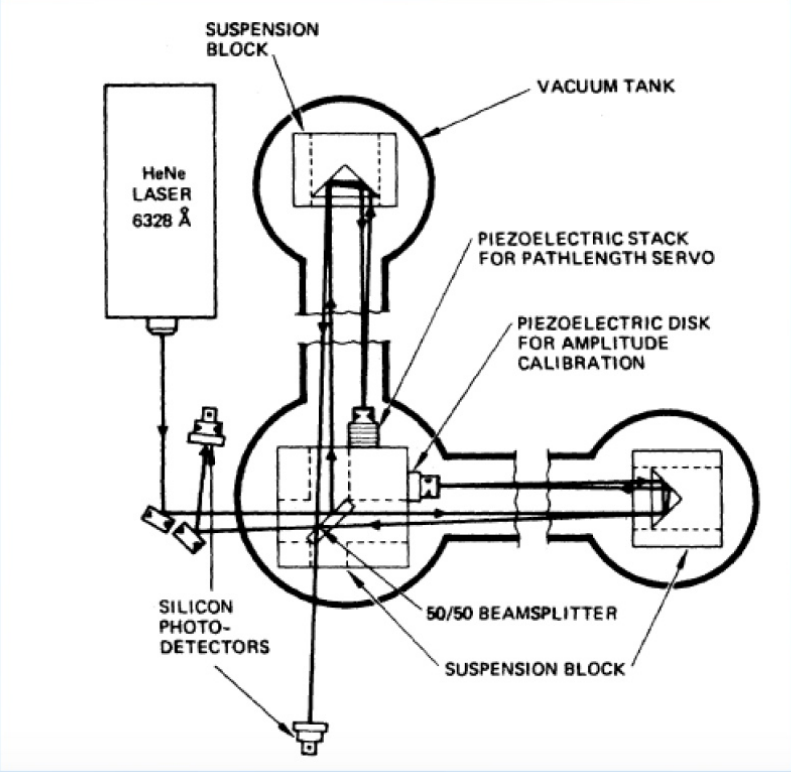

VII. CALIBRATION OF EAR

When the interferometer was working well, we were able to hear single-frequency 3- to 10-kHz tones of 10-fm rms amplitude introduced into the interferometer by the piezoelectric displacement transducer.

Since the noise level of the interferometer in that band is about 0.9 fm/$Hz^{1/2}$, this means that the audio system, including our ear-brain combination, had an effective detection bandwidth of about 120 Hz.

Rai Weiss Interferometer Study

1972: Weiss produces the first detailed study for a realistic interferometric gravitational wave detector.

Systematically addresses a number of realistic noise sources:

- Amplitude Noise in the Laser Output Power
- Laser Phase Noise or Frequency Instability
- Mechanical Thermal Noise in the Antenna
- Radiation-Pressure Noise from the Laser Light
- Seismic Noise
- Thermal-Gradient Noise
- Cosmic-Ray Noise
- Gravitational-Gradient Noise
- Electric Field and Magnetic Field Noise

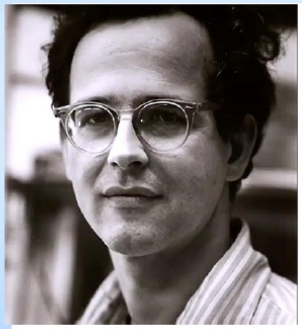

Fig. V-20. Proposed antenna.

Prototype Interferometric Detectors

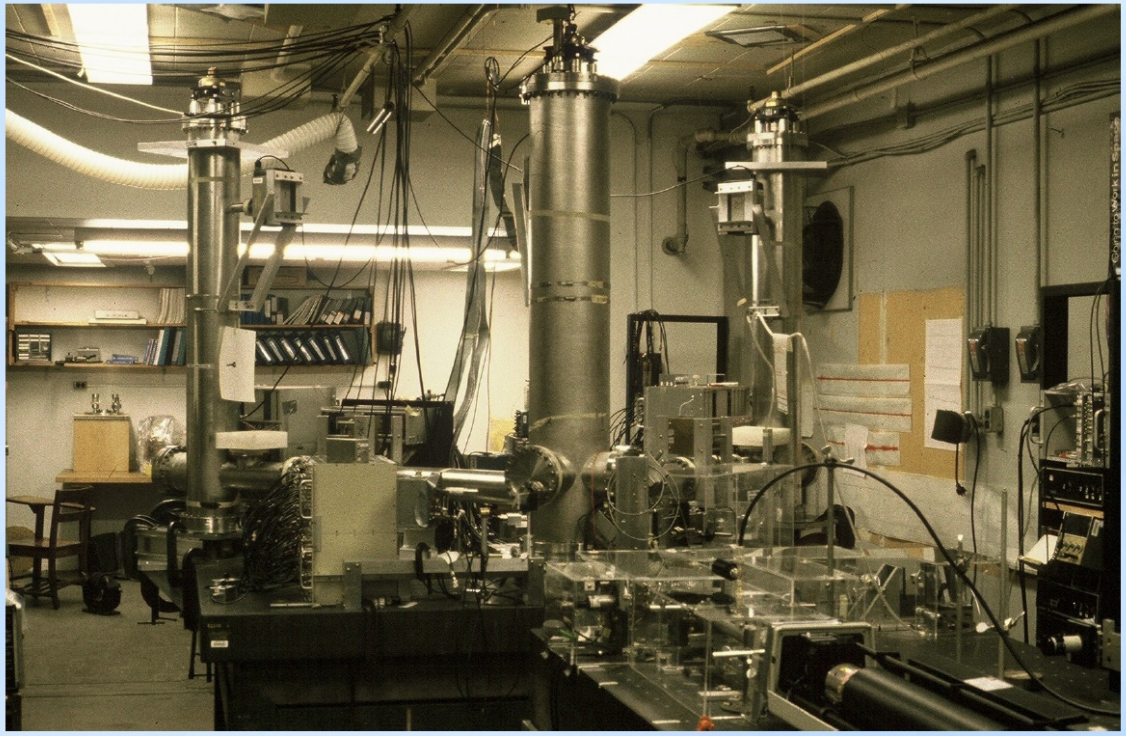

MIT 1.5 m delay line Michelson Interferometer

1970s and 80s:
Interferometers constructed at
Garching
Glasgow
MIT
Caltech

The interferometer technology started progressing rapidly.

1980s LIGO is Born

Thorne, Drever (Caltech)

Weiss (MIT)

National Science Foundation

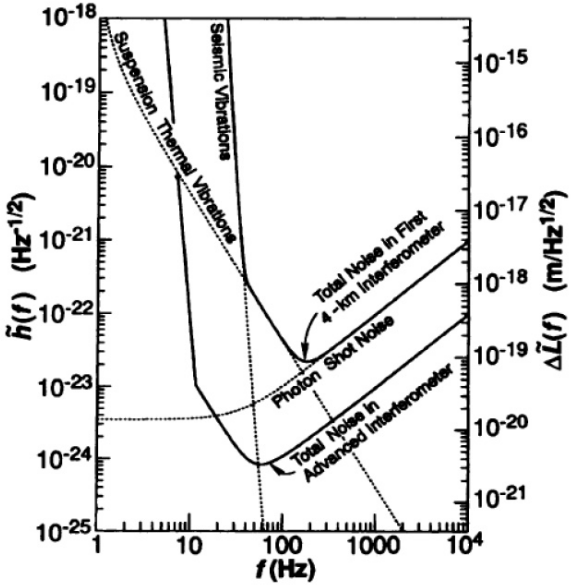

Fig. 7. The expected total noise in each of LIGO's first 4-km interferometers (upper solid curve) and in a more advanced interferometer (lower solid curve). The dashed curves show various contributions to the first interferometer's noise.

SCIENCE • VOL. 256 • 17 APRIL 1992

While in Europe … Virgo

A. Brillet (Orsay, Nice)
Lasers, Optics

A. Giazotto (Pisa)
Vibration Isolation

cnrs

INFN

The Detectors

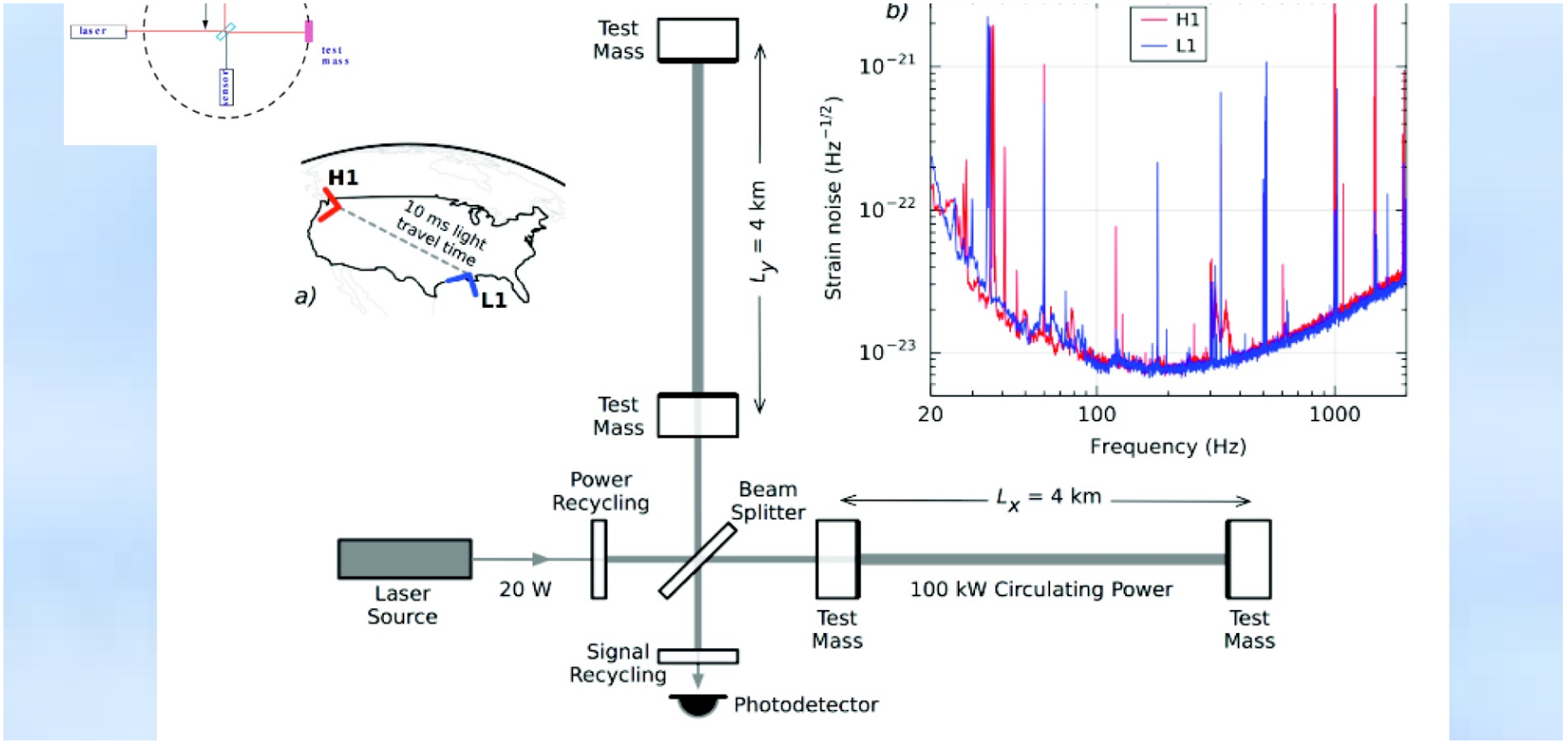

Advanced LIGO – Advanced Virgo

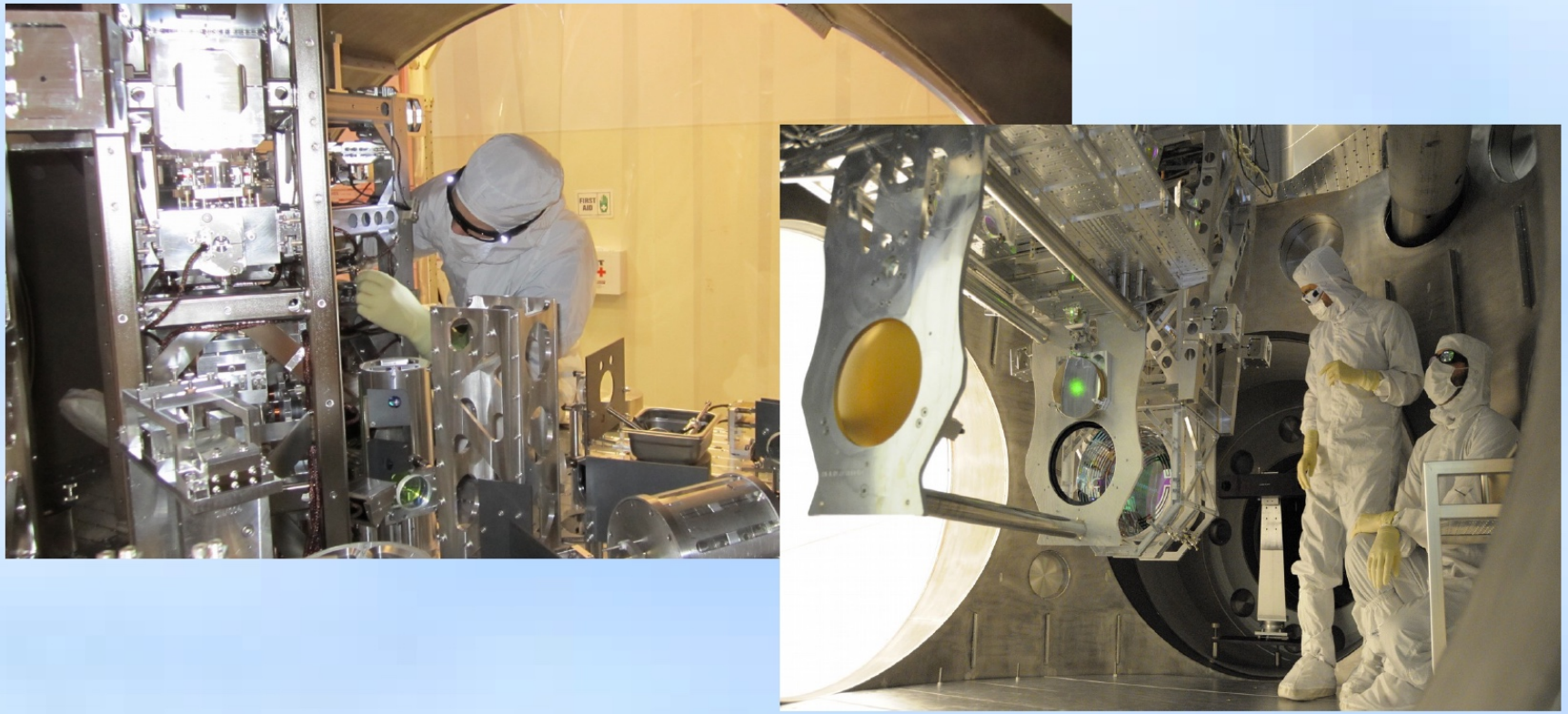

Built on the experience gained from the first generation detectors

Advanced LIGO

- Advanced LIGO commissioned 2010-2015.
  - » Increased laser power
  - » Sophisticated seismic/vibration suppression
  - » Quadruple pendula suspensions
  - » Larger mirrors, better suspension material
  - » More complex and versatile interferometer configuration.

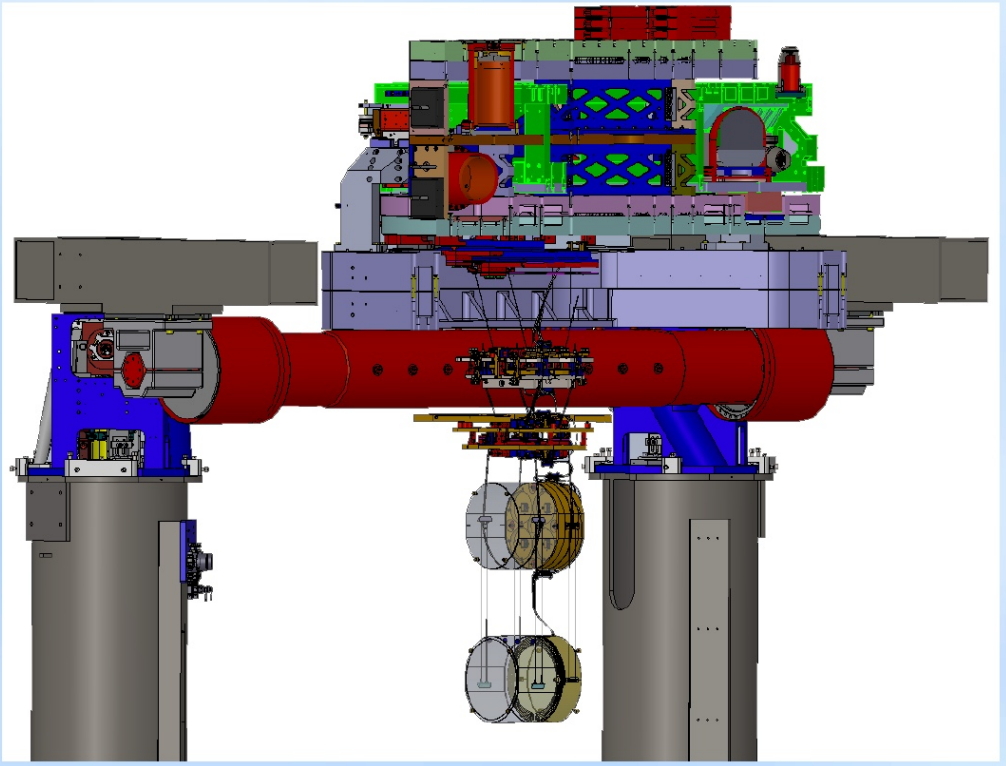

Advanced Virgo

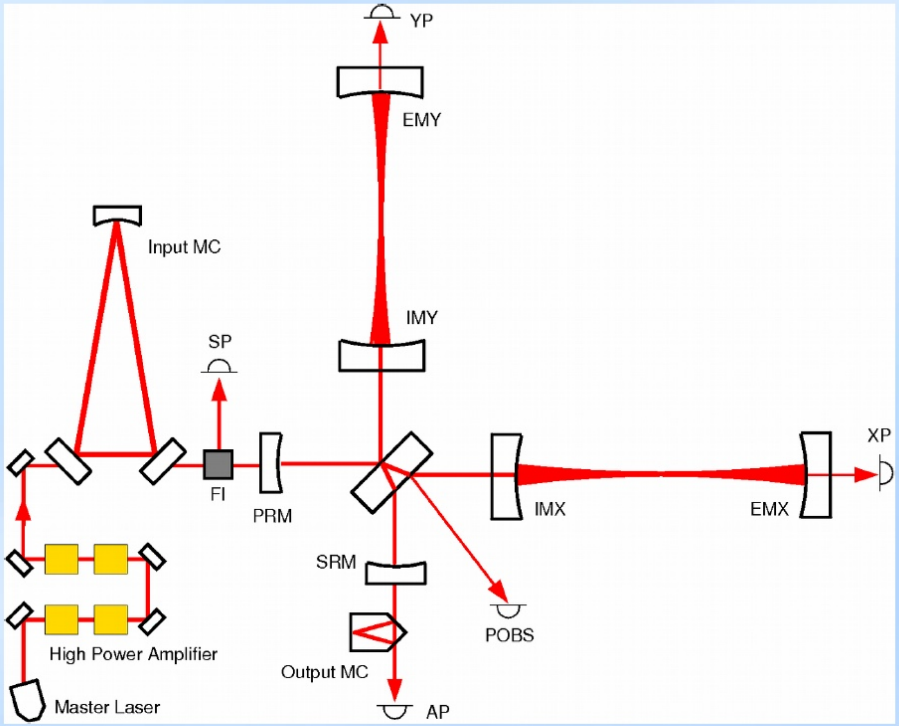

- Larger mirrors; better optical quality.
- Higher finesse of the arm cavities
- Increased laser power.
- Coming on-line in Spring 2017.

Advanced Virgo

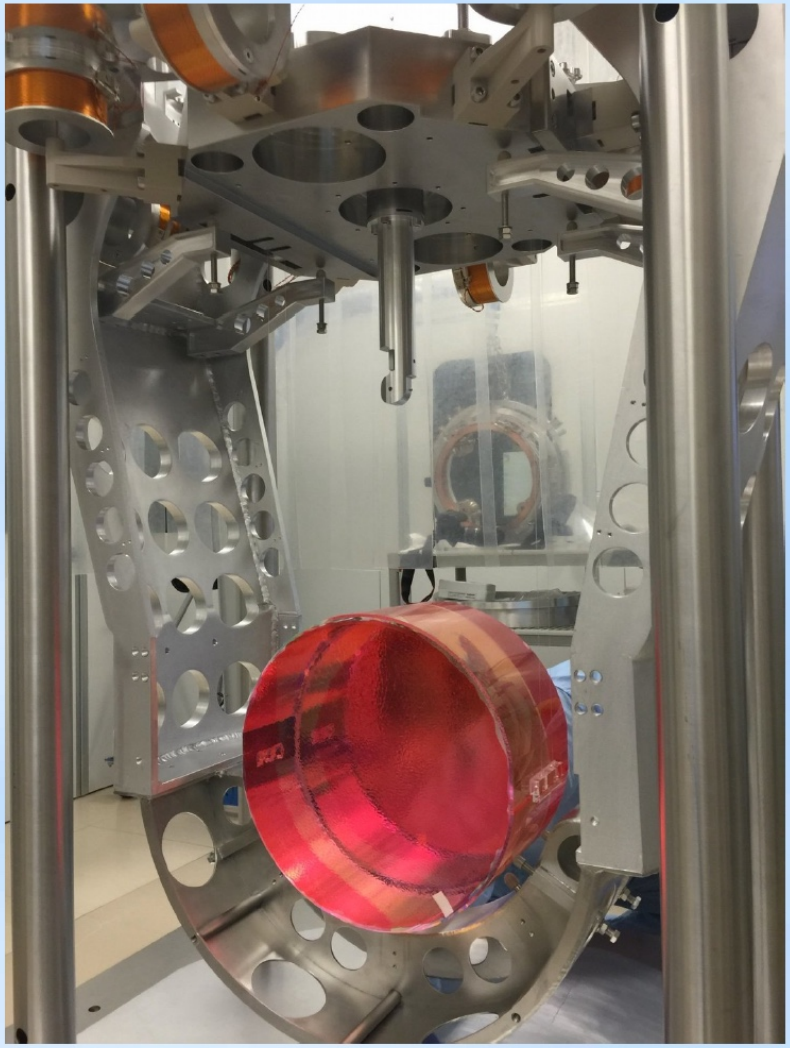

Mirror

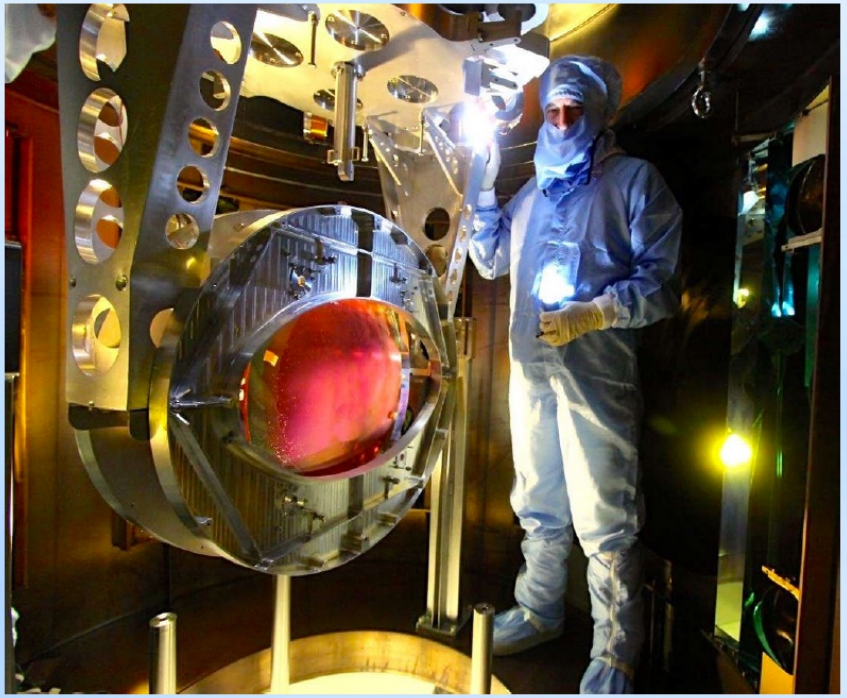

Beamsplitter

The optical components are very large, but their quality is exquisite.

GW150914

- Band-pass filter:
  35-350 Hz
- L1-H1 time delay of about 7ms.
- Chirp signal, typical of binary coalescences.
- Detected by online burst-search pipelines.
- Confirmed later matched template searches.
- Combined SNR: 24.

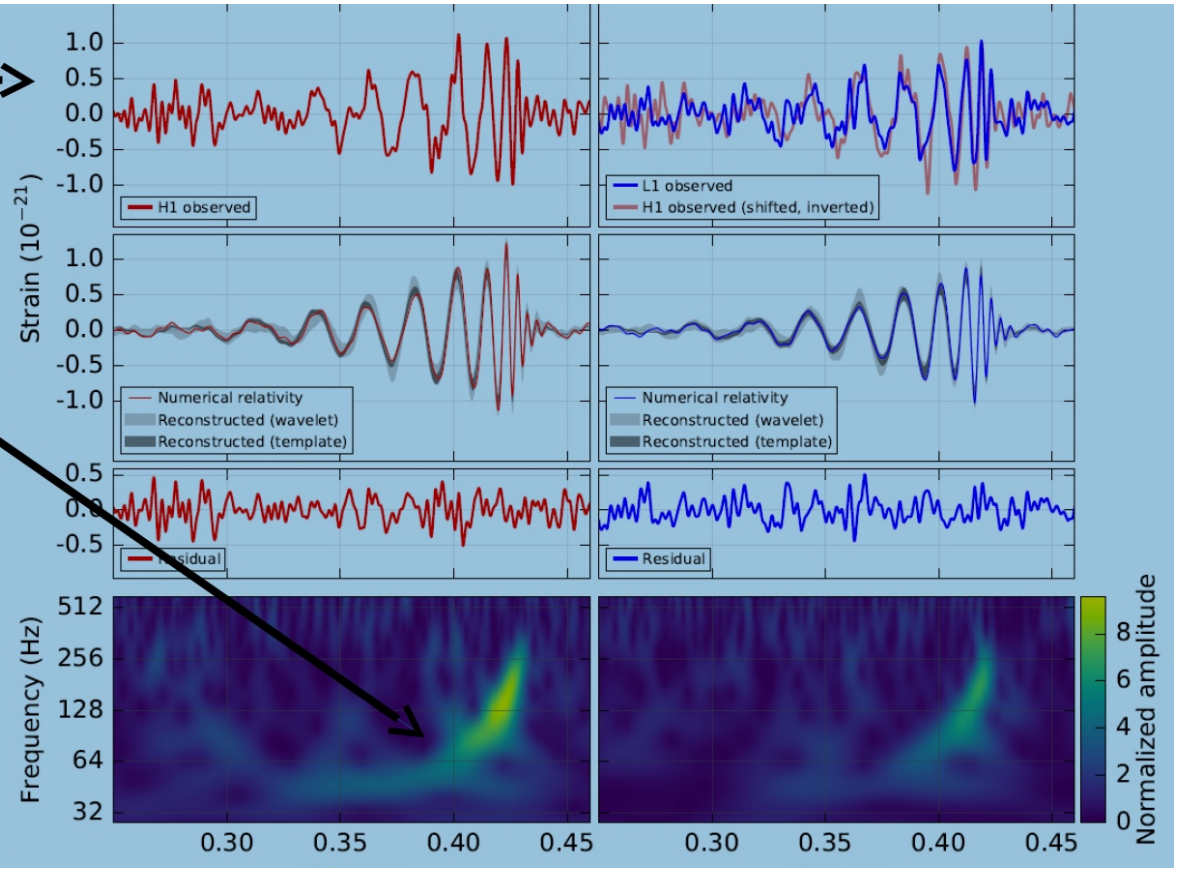

The Results

Observation of Gravitational Waves from a Binary Black Hole Merger

B. P. Abbott *et al.*[*]
(LIGO Scientific Collaboration and Virgo Collaboration)
(Received 21 January 2016; published 11 February 2016)

On September 14, 2015 at 09:50:45 UTC the two detectors of the Laser Interferometer Gravitational-Wave Observatory simultaneously observed a transient gravitational-wave signal. The signal sweeps upwards in frequency from 35 to 250 Hz with a peak gravitational-wave strain of 1.0×10^{-21}. It matches the waveform predicted by general relativity for the inspiral and merger of a pair of black holes and the ringdown of the resulting single black hole. The signal was observed with a matched-filter signal-to-noise ratio of 24 and a false alarm rate estimated to be less than 1 event per 203 000 years, equivalent to a significance greater than 5.1σ. The source lies at a luminosity distance of 410^{+160}_{-180} Mpc corresponding to a redshift $z = 0.09^{+0.03}_{-0.04}$. In the source frame, the initial black hole masses are $36^{+5}_{-4}M_{\odot}$ and $29^{+4}_{-4}M_{\odot}$, and the final black hole mass is $62^{+4}_{-4}M_{\odot}$, with $3.0^{+0.5}_{-0.5}M_{\odot}c^2$ radiated in gravitational waves. All uncertainties define 90% credible intervals. These observations demonstrate the existence of binary stellar-mass black hole systems. This is the first direct detection of gravitational waves and the first observation of a binary black hole merger.

DOI: 10.1103/PhysRevLett.116.061102

Primary black hole mass	$36^{+5}_{-4}M_{\odot}$
Secondary black hole mass	$29^{+4}_{-4}M_{\odot}$
Final black hole mass	$62^{+4}_{-4}M_{\odot}$
Final black hole spin	$0.67^{+0.05}_{-0.07}$
Luminosity distance	410^{+160}_{-180} Mpc
Source redshift z	$0.09^{+0.03}_{-0.04}$

Phenomenology of GW

When GW passes through space deforms it

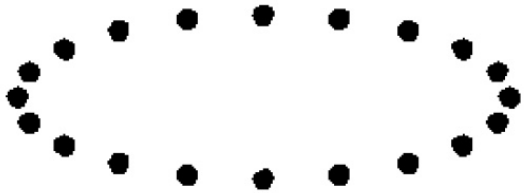

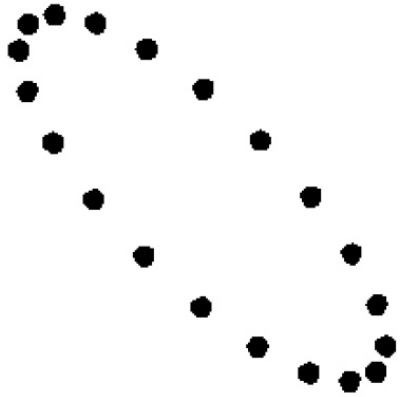

When GW passes through space deforms it

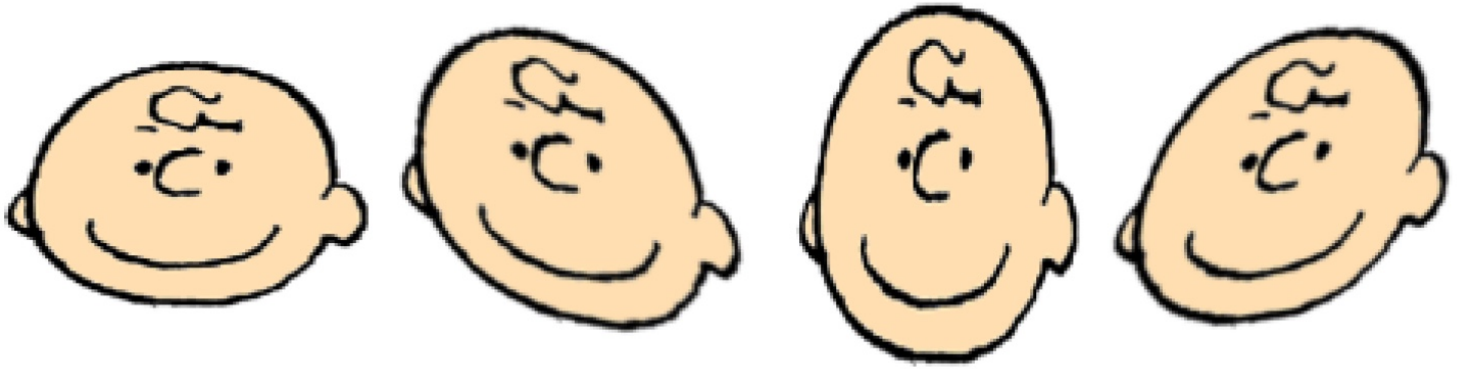

When GW passes through space deforms it

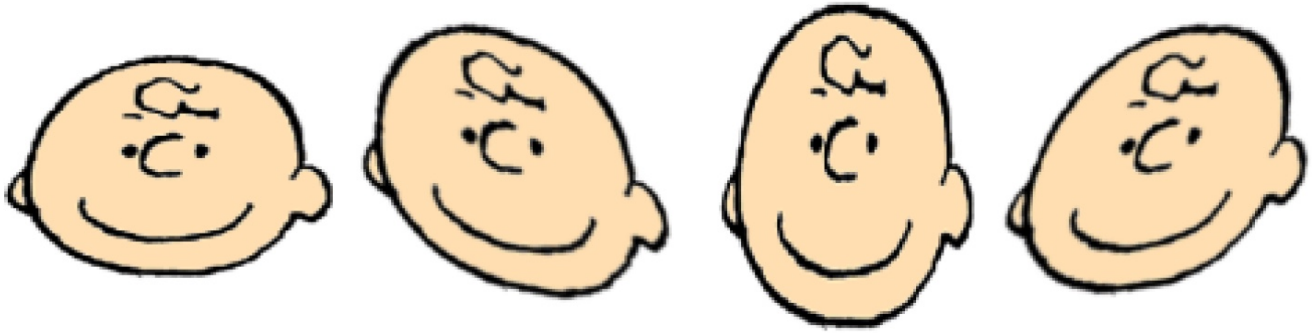

But deformations are very small: strain=relative deformation

$$h = DL/L \sim 1e\text{-}21$$

For $L_{Sun\text{-}Earth} \sim 1.5e13$ cm

$h\, L_{Sun\text{-}Earth} \sim 1e\text{-}21 \times 1.5e13 \sim 1.5e\text{-}08$cm

size of H atom at distance Sun-Earth

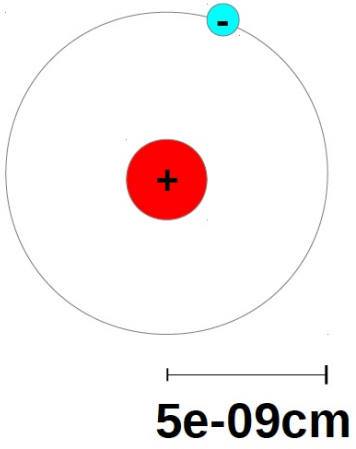

Some math:

Consider Einstein equation

$$R_{\mu\nu} - \frac{1}{2} g_{\mu\nu} R = \frac{8\pi G}{c^4} T_{\mu\nu}$$

Consider a small perturbation of the flat Cartesian metric
Weak field (far from source)

$$g_{\mu\nu} = \eta_{\mu\nu} + h_{\mu\nu} \qquad with\, |h_{\mu\nu}| \ll 1$$

Using gauge invariance and assuming vacuum (*T*=0 no mass no energy)

Equation of WAVES!!

$$\Box h = -\frac{16\pi G}{c^4} T_{\mu\nu} = 0$$

If you want to know more about GR formalism:
https://arxiv.org/pdf/1607.04202.pdf

By integrating equation $\Box h = -\frac{16\pi G}{c^4} T_{\mu\nu}$

$$h^{ij}(t,\vec{x}) \sim \frac{2\,G}{r\,c^4}\frac{d^2}{dt^2} I^{ij}(t - r/c)$$

Distance source-observer

Moment of inertia, or second mass moment, or quadrupole moment of mass $I^{ij} = \int dx^3\, \rho(t,\vec{x})\, x^i\, x^j$

Retarded time

→ **not all accelerating masses do this job but only those with <u>QUADRUPOLE</u>**

If you do calculation, monopole and dipole disappear

→ **for a gravitational wave to form, there must be an ASYMMETRY IN MASS DISTRIBUTION**

What are the astrophysical objects with non-zero quadrupole?

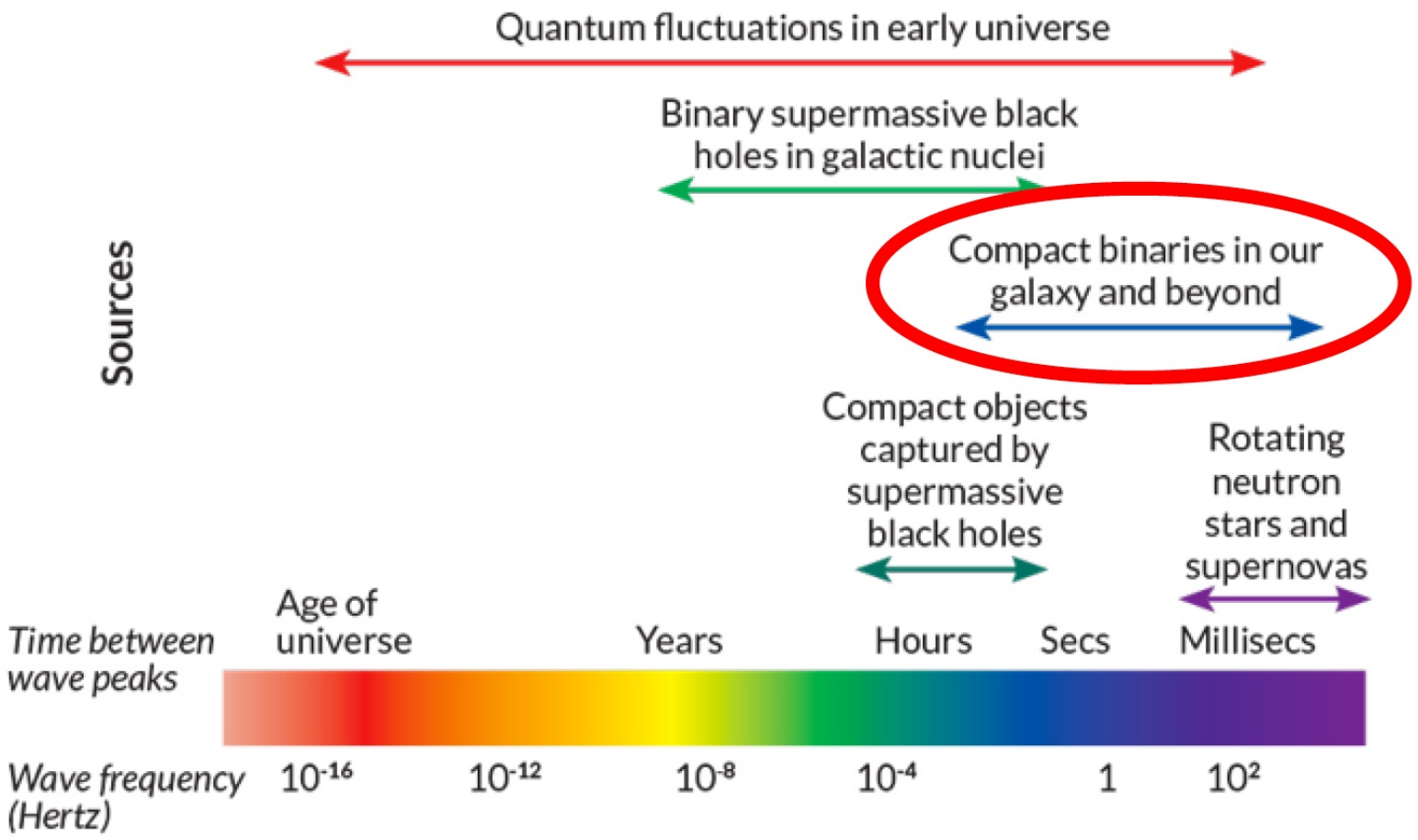

Primordial gravitational waves / Quantum fluctuations:

<< 1 sec from Big Bang, due to INFLATION of the Universe
Freq. ~ 10^-16 – 10^2 Hz
extremely “faint” (small amplitude)

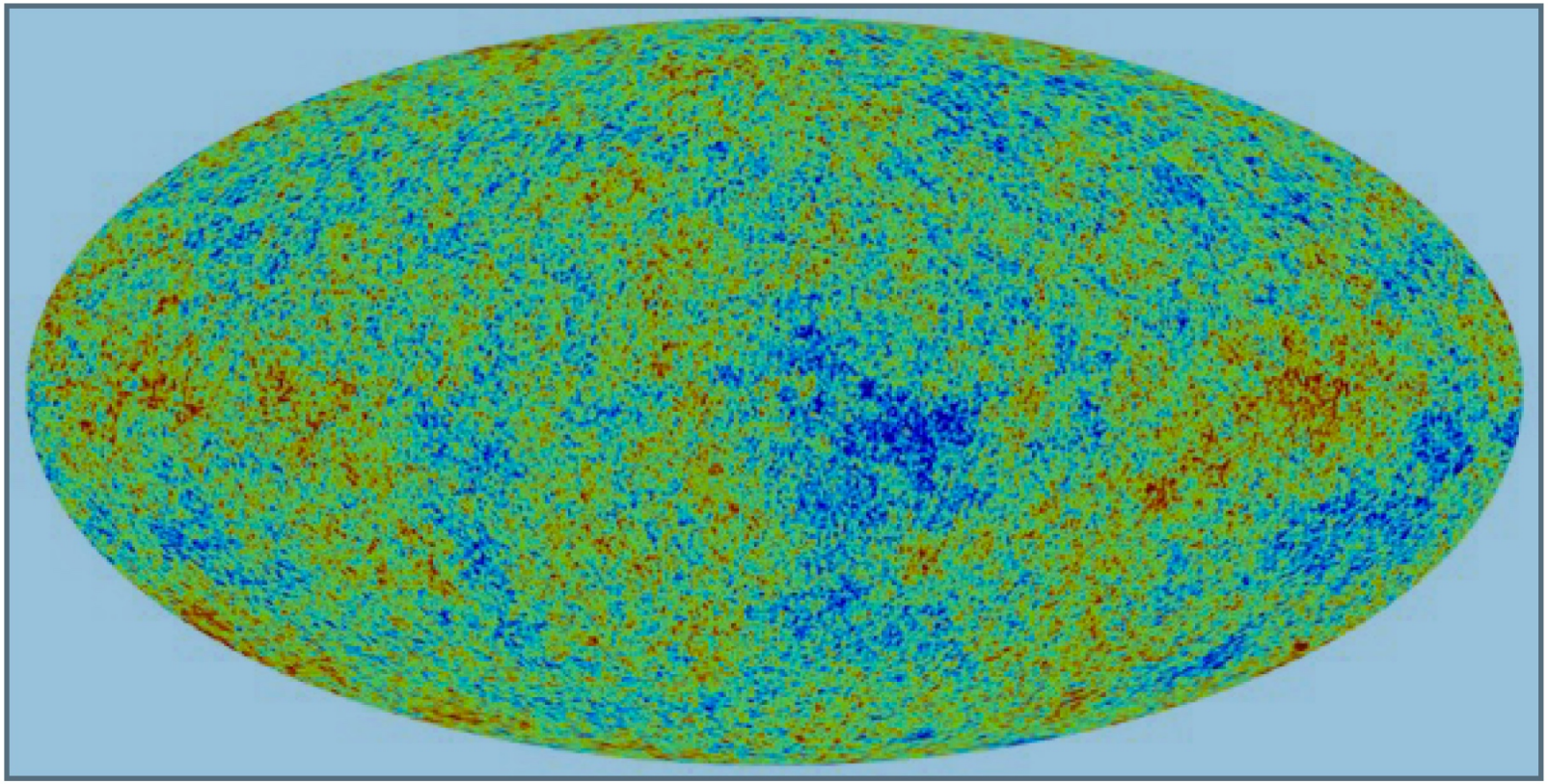

Mergers of super-massive black holes (SMBHs, >10^5 Msun):

Black holes at centre of galaxies might form Keplerian binaries and might merge

Freq. ~ 10^-10 – 0.1 Hz

Mergers of super-massive black holes (SMBHs, >10^5 Msun):

Black holes at centre of galaxies might form Keplerian binaries and might merge

Freq. ~ 10^-10 – 0.1 Hz

Mergers of compact object binaries (black holes <10^5 Msun, neutron stars):

Black holes (BHs) and neutron stars (NSs) born from stars might merge
Freq. ~ 10^-4 – 10^3 Hz

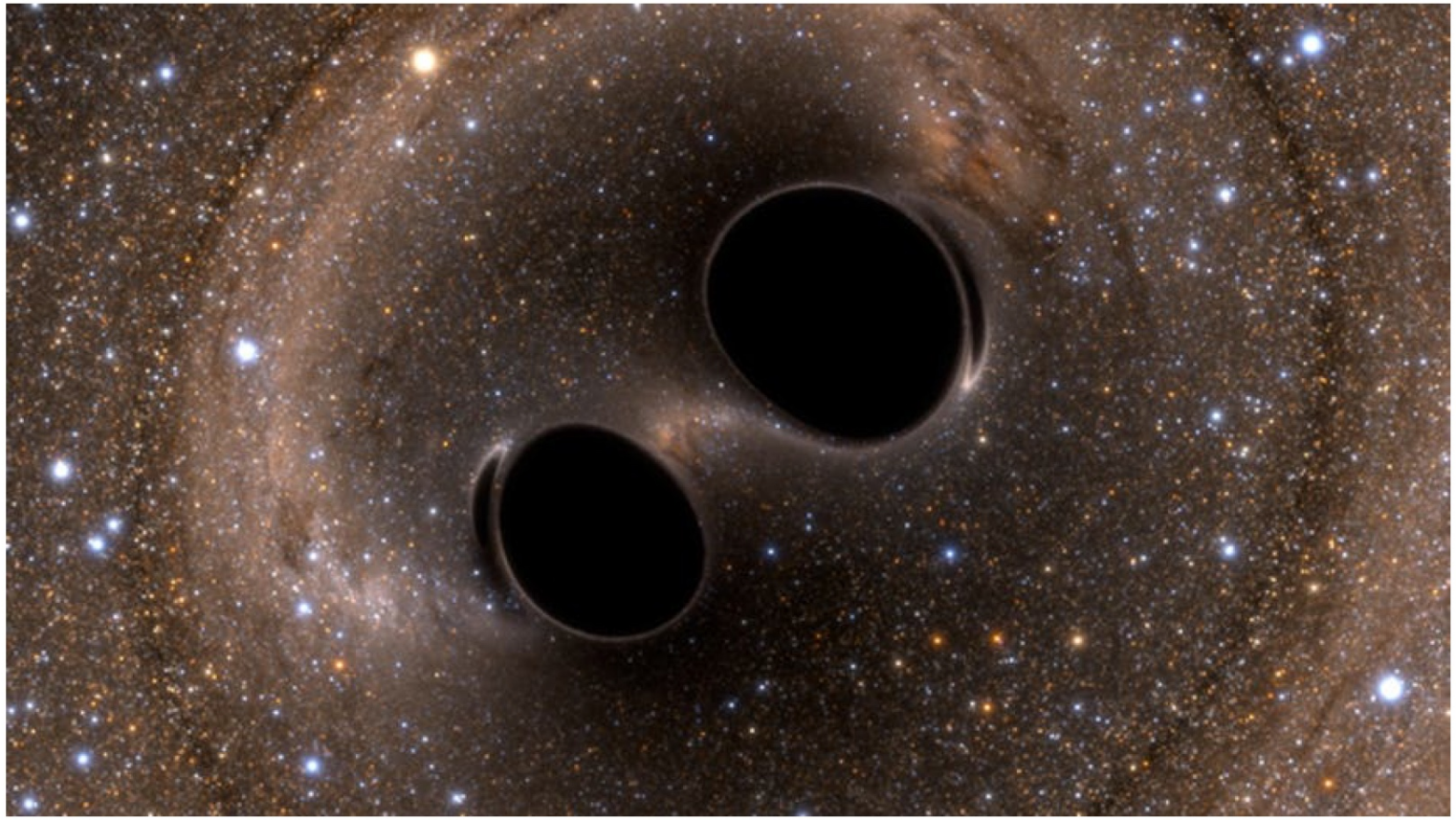

Mergers of SMBHs and stellar-mass BHs:

Small BHs might orbit SMBHs and be captured by them

Freq. ~ 10^-4 – 0.1 Hz

Mergers of SMBHs and stellar-mass BHs:

Small BHs might orbit SMBHs and be captured by them

Freq. ~ 10^-4 – 0.1 Hz

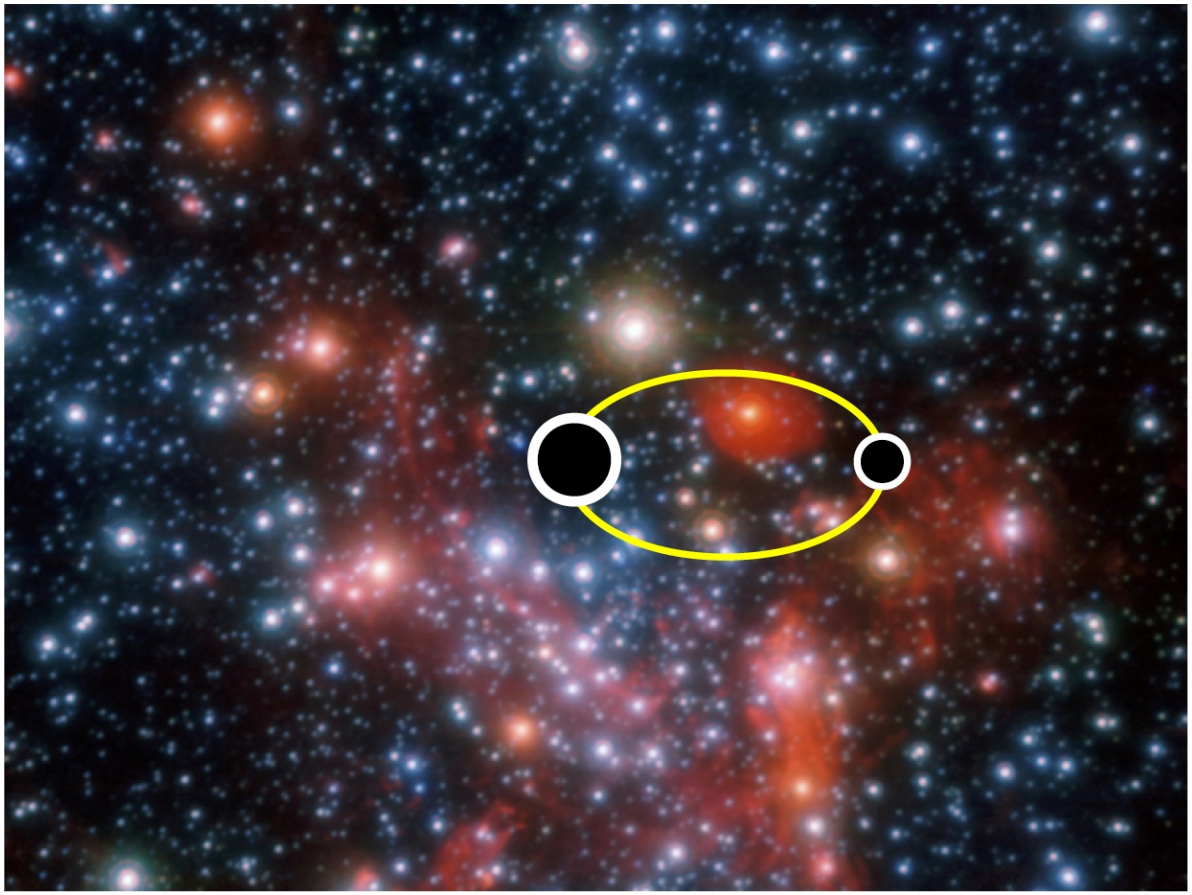

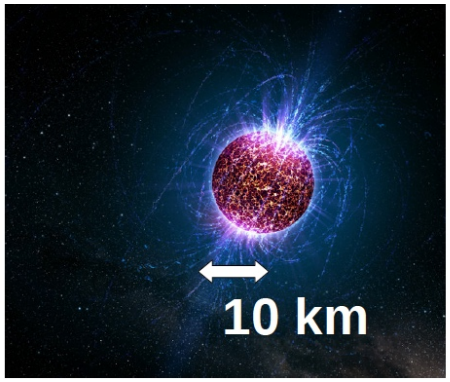

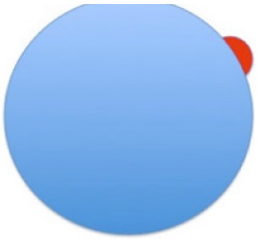

Asymmetric supernova explosions:
Freq. ~ 10 – 10^2 Hz

Mergers of super-massive black holes (SMBHs, >10^5 Msun)

Mergers of compact object binaries

Only GWs observed so far

Mergers of SMBHs and BHs

Neutron stars with crustal asymmetries

Asymmetric supernova explosions

Some essential math about GWs from BINARIES:

It can be shown that $$h^{ij}(t,\vec{x}) \sim \frac{2\,G}{r\,c^4}\frac{d^2}{dt^2}\,I^{ij}(t-r/c)$$

can be expressed in spherical coordinates (*r, ϕ, θ*)
for a KEPLERIAN BINARY with reduced mass μ = *m1 m2/(m1+m2)*
with semi-major axis *a*, with orbital frequency ω_{orb}
and eccentricity *e* = 0 as

$$h_+(t,\theta,\phi,r) = \frac{1}{r}\,\frac{4\,G\,\mu\,\omega_{orb}^2\,a^2}{c^4}\,\frac{1+\cos^2\theta}{2}\,\cos\left(2\,\omega_{orb}\,t_{ret}+\phi\right)$$

$$h_x(t,\theta,\phi,r) = \frac{1}{r}\,\frac{4\,G\,\mu\,\omega_{orb}^2\,a^2}{c^4}\,\cos\theta\,\sin\left(2\,\omega_{orb}\,t_{ret}+\phi\right)$$

where $t_{ret} = t - r/c$ $\qquad$ $\omega_{orb}^2 = \frac{G\,(m_1+m_2)}{a^3}$

This equation tells us:

– **GWs are POLARIZED (h_+, h_x)**

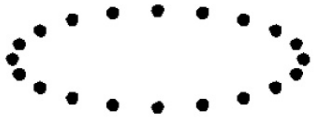

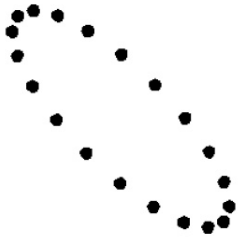

– **FREQUENCY TERM DEPENDS only ON $2\,\omega_{orb}$**

→ **frequency of GWs $\omega_{GW} = 2\,\omega_{orb}$**

(true for most evolution)

– **AMPLITUDE of GWs:**

$$h = \frac{1}{2}\sqrt{h_+^2 + h_x^2} = \frac{2\,G\,\mu\,\omega_{orb}^2\,a^2}{c^4}\,\frac{1}{r}\sqrt{\frac{(1+\cos^2\theta)^2}{4} + cos^2\theta}$$

$$h = \frac{1}{2}\sqrt{h_+^2 + h_x^2} = \frac{2\,G^2\,m_1\,m_2}{a\,c^4}\,\frac{1}{r}\sqrt{\frac{(1+\cos^2\theta)^2}{4} + cos^2\theta}$$

– **AMPLITUDE of GWs:**

$$h = \frac{1}{2}\sqrt{h_+^2 + h_x^2} = \frac{2\,G^2\,m_1\,m_2}{a\,c^4}\,\frac{1}{r}\,\sqrt{\frac{(1+\cos^2\theta)^2}{4} + cos^2\theta}$$

*** the bigger the amplitude (strain), the easier the detection**

*** the farther the binary, the smaller the amplitude**

*** the larger the masses, the larger the amplitude**

*** the smaller the semi-major axis, the larger the amplitude**

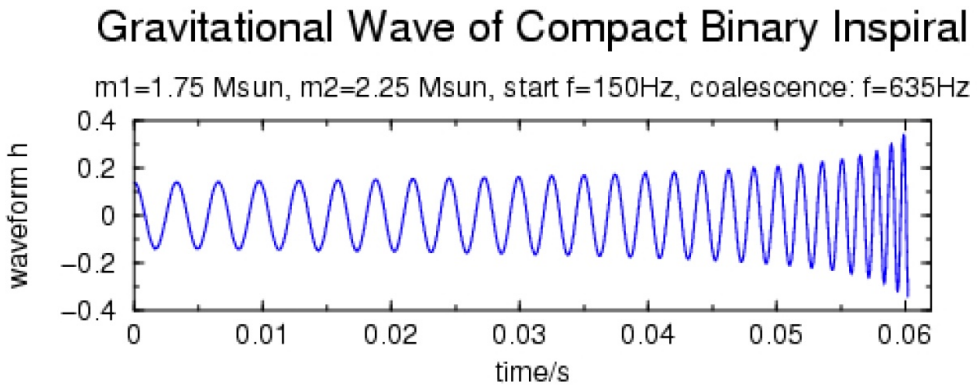

– EMISSION of GWs implies LOSS of ORBITAL ENERGY:

$$E_{orb} = -\frac{G\, m_1\, m_2}{2\, a}$$

THE BINARY SHRINKS WHILE EMITTING GWs
TILL IT MERGES

https://www.youtube.com/watch?v=g8s81MzzJ5c

– **EMISSION of GWs implies LOSS of ORBITAL ENERGY:**
THE BINARY SHRINKS WHILE EMITTING GWs
TILL IT MERGES

– **If the binary shrinks ($a \rightarrow 0$), frequency becomes higher**

– **If the binary shrinks amplitude increases**

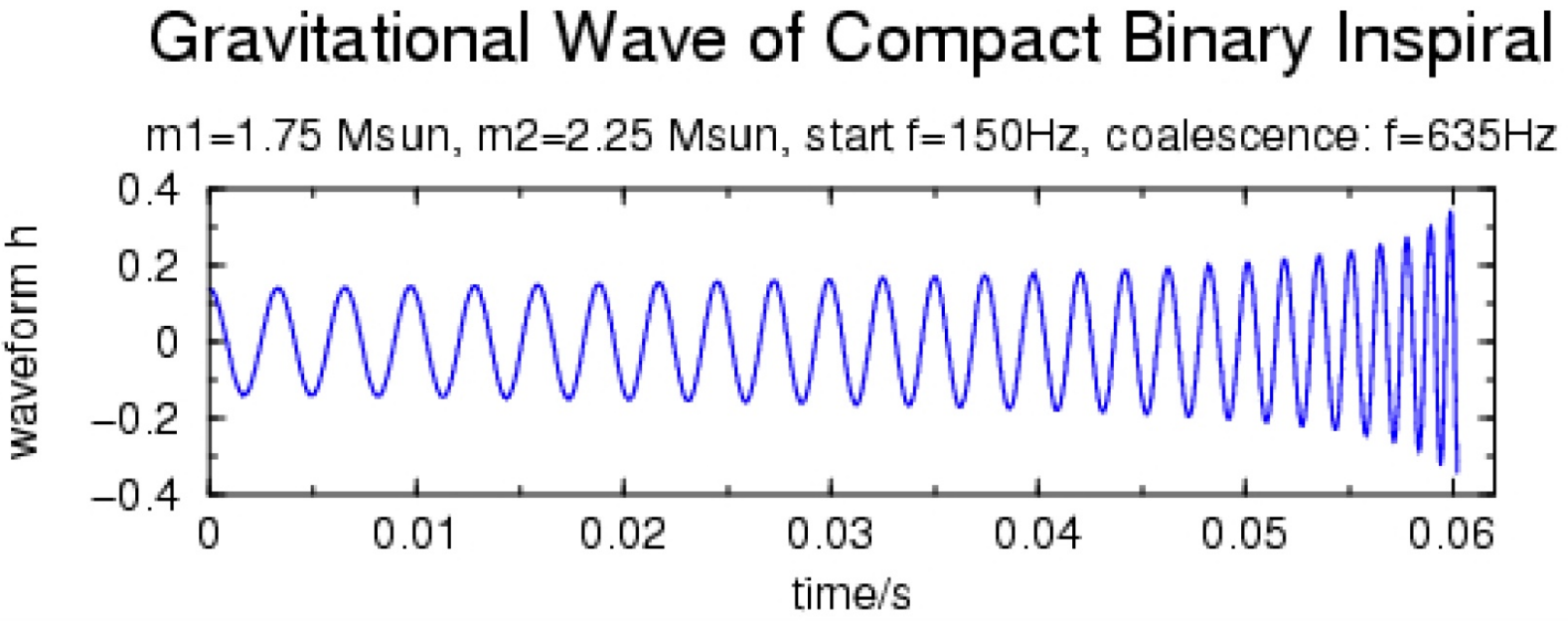

– **EMISSION of GWs implies LOSS of ORBITAL ENERGY:**

Power radiated by GWs:

From GR

$$P_{GW} = \frac{32}{5}\frac{G^4}{c^5}\frac{1}{a^5}\,m_1^2\,m_2^2\,(m_1+m_2)$$

$$P_{GW} = \frac{dE_{orb}}{dt} = \frac{G\,m_1\,m_2}{2\,a^2}\frac{da}{dt}$$

From Kepler and Newton

$$\frac{da}{dt} = \frac{64}{5}\frac{G^3}{c^5}\,a^{-3}\,m_1\,m_2\,(m_1+m_2)$$

Integrating differential equation:

$$t_{GW} = \frac{5}{256}\frac{c^5}{G^3}\frac{a^4}{m_1\,m_2\,(m_1+m_2)}$$

Timescale for a system to merge by GW emission

For binaries with general eccentricity e

$$t_{GW} = \frac{5}{256}\,\frac{c^5}{G^3}\,\frac{a^4\,(1-e^2)^{7/2}}{m_1\,m_2\,(m_1+m_2)}$$

Peters 1964

Timescale depends on semi-major axis, eccentricity, masses

Timescale extremely long

EXERCISE: calculate tGW for 2 neutron stars with mass equal to the Sun mass (1 Msun) orbiting at the distance between Sun and Earth (1 AU)

$$a(t) = a_0 \left[1 - \frac{256/5\, G^3\, m_1\, m_2\, (m_1 + m_2)\, t}{c^5\, (1 - e^2)^{7/2}\, a_0^4} \right]^{1/4}$$

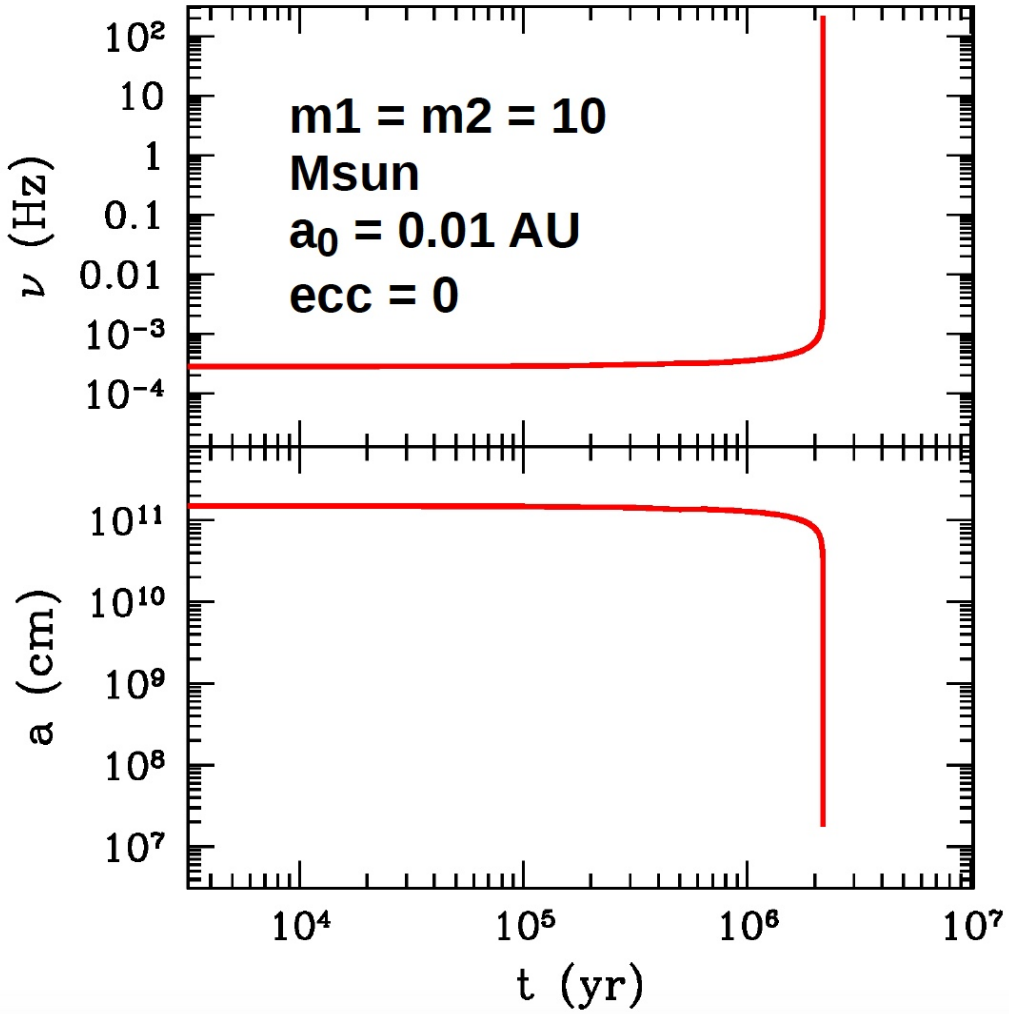

Previous equations are not always true!

Only before merger when binary can be considered Keplerian

i.e. only during inspiral

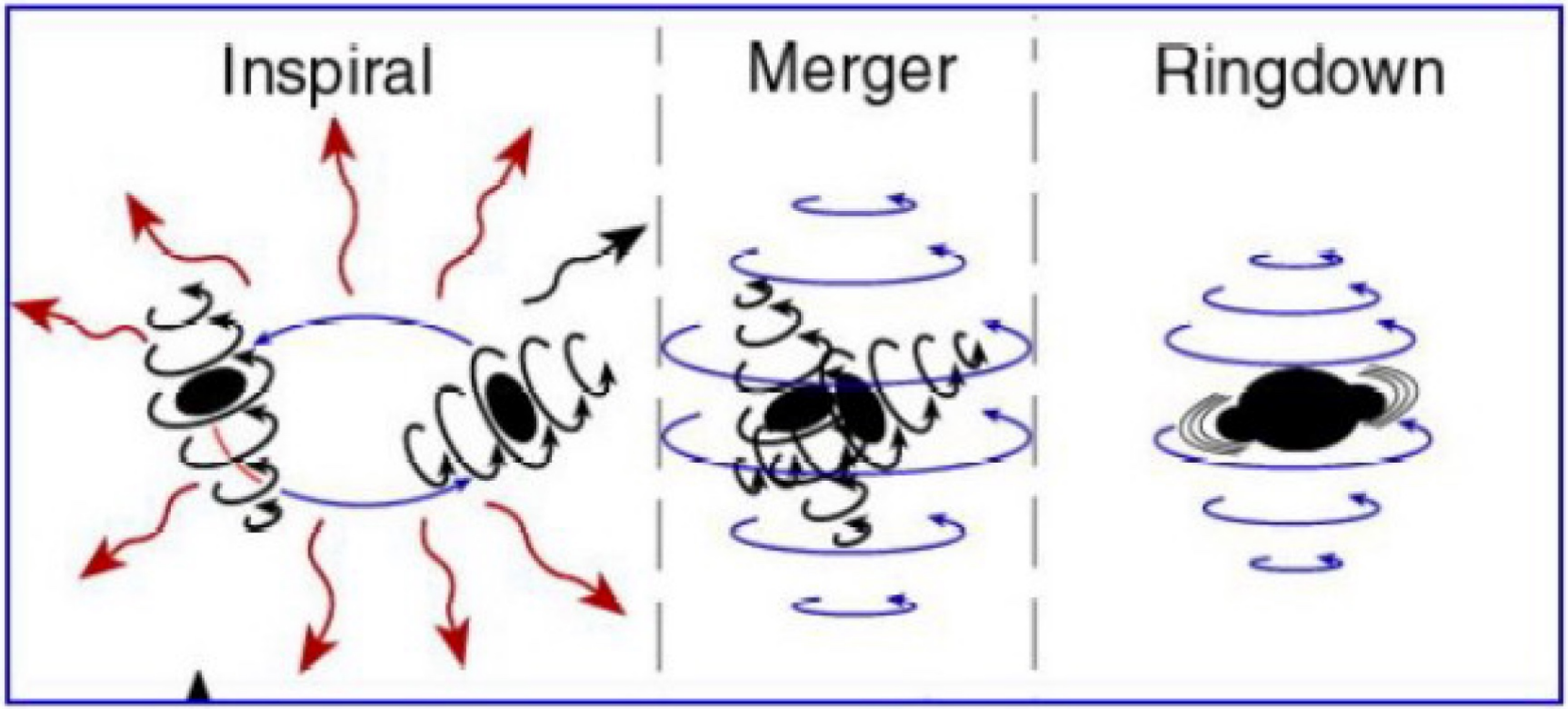

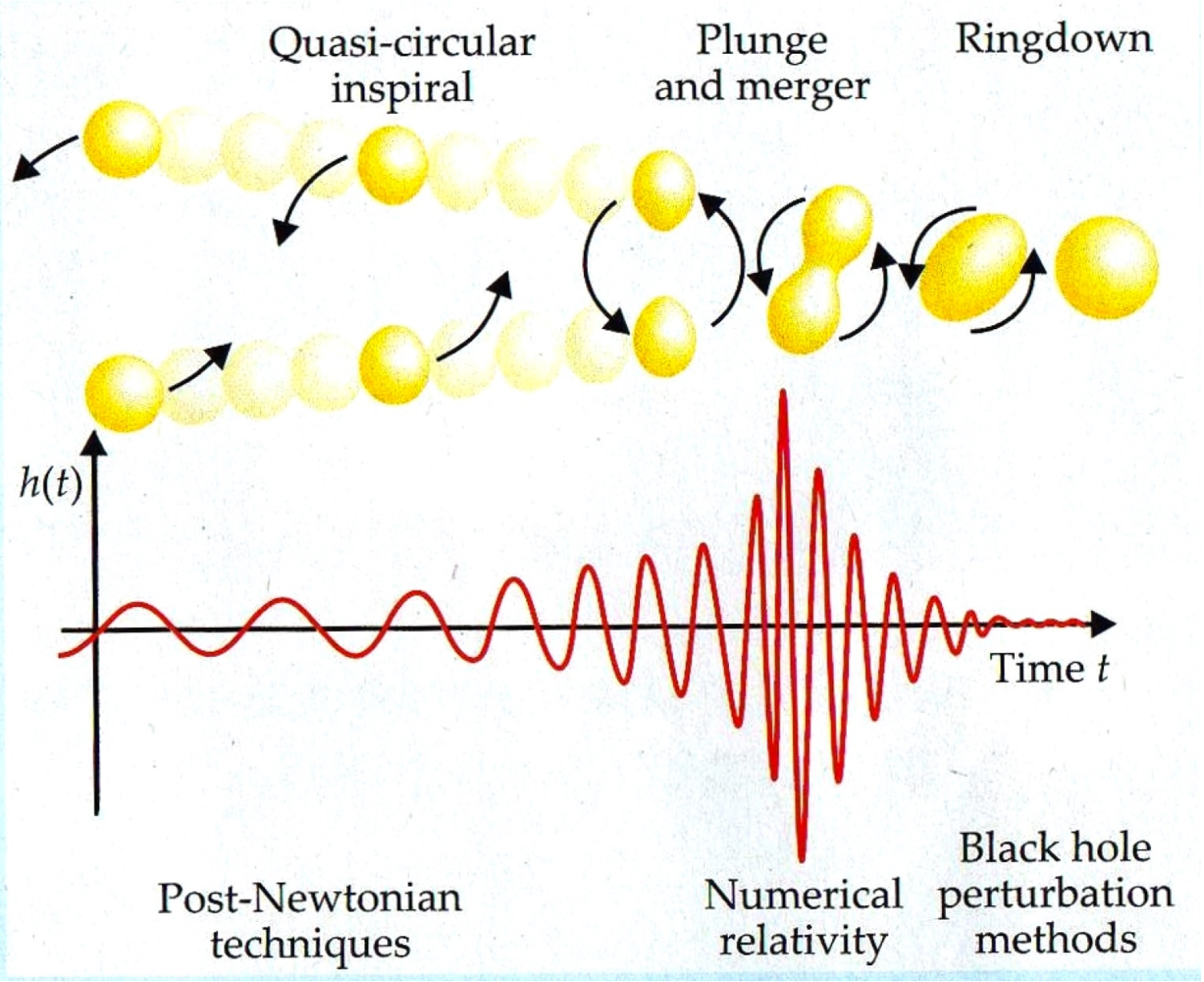
Quasi-circular inspiral
Plunge and merger
Ringdown
h(t)
Time t
Post-Newtonian techniques
Numerical relativity
Black hole perturbation methods

Templates for GWs from BBH coalescence

(Brady, Craighton, Thorne 1998)

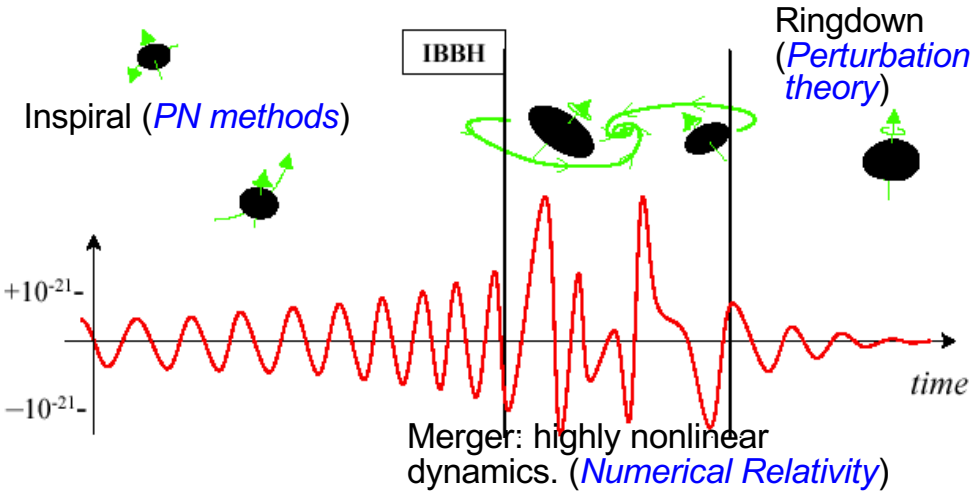

(Buonanno & Damour 2000)

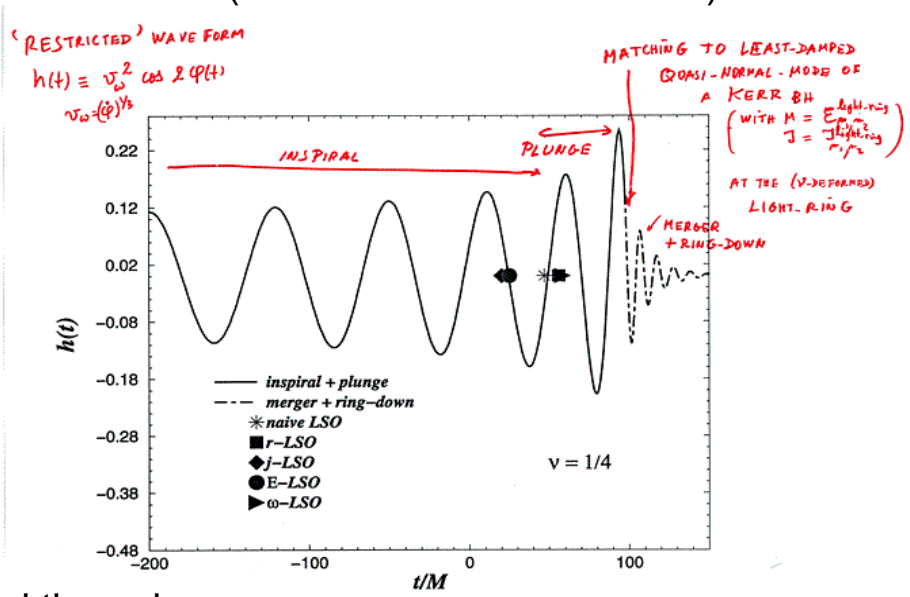

Numerical Relativity, the 2005 breakthrough:
Pretorius, Campanelli et al., Baker et al. …

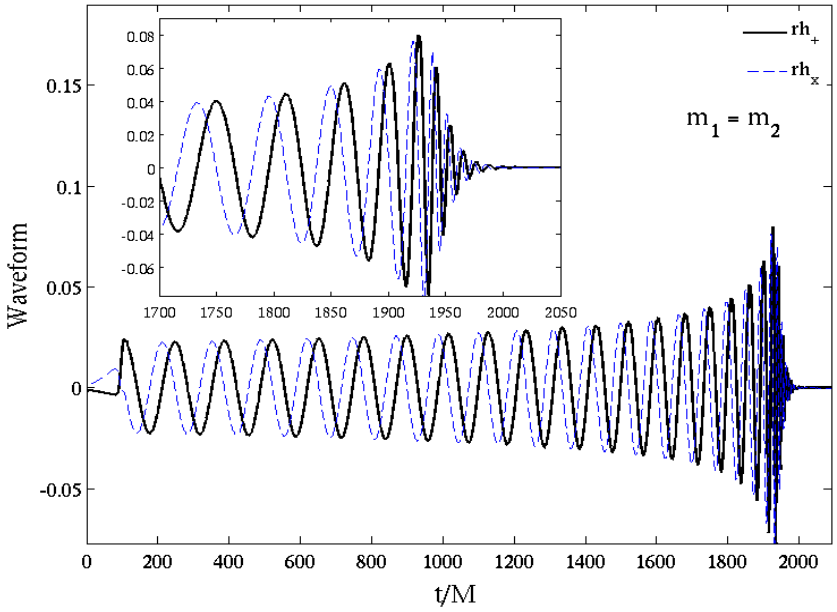

NUMERICAL RELATIVITY WAVEFORM

Numerical Relativity: >= 2005 (Pretorius, Campanelli et al., Baker et al.)

Very accurate data: Caltech-Cornell spectral code (with some caveats): M. Scheel et al., 2008

Spectral code

Extrapolation (radius & resolution) Phase error: < 0.02 rad (inspiral) <0.1 ra (ringdown)

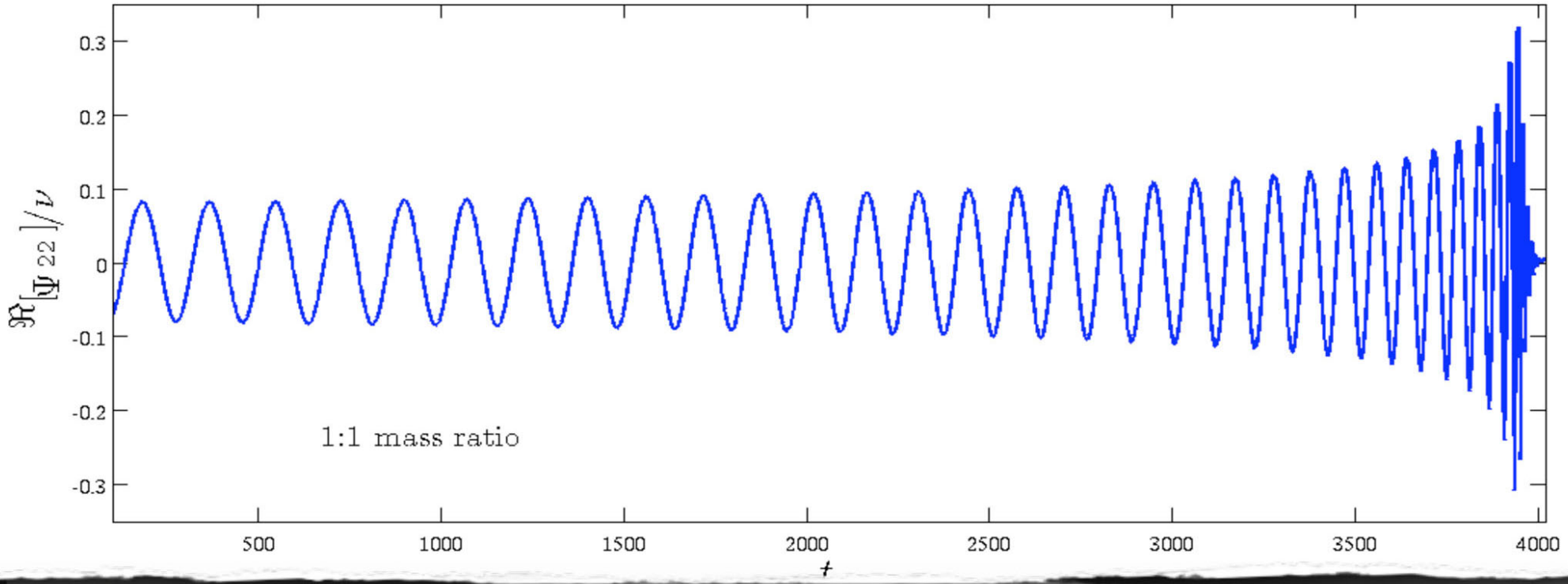

Importance of an analytical formalism

- **Theoretical:** physical understanding of the coalescence process, especially in complicated situations (arbitrary spins)
- **Practical:** need many thousands of accurate GW templates for detection & data analysis;
  need some "analytical" representation of waveform templates as $f(m_1, m_2, \mathbf{S_1}, \mathbf{S_2})$
- Solution: **synergy between analytical & numerical relativity**

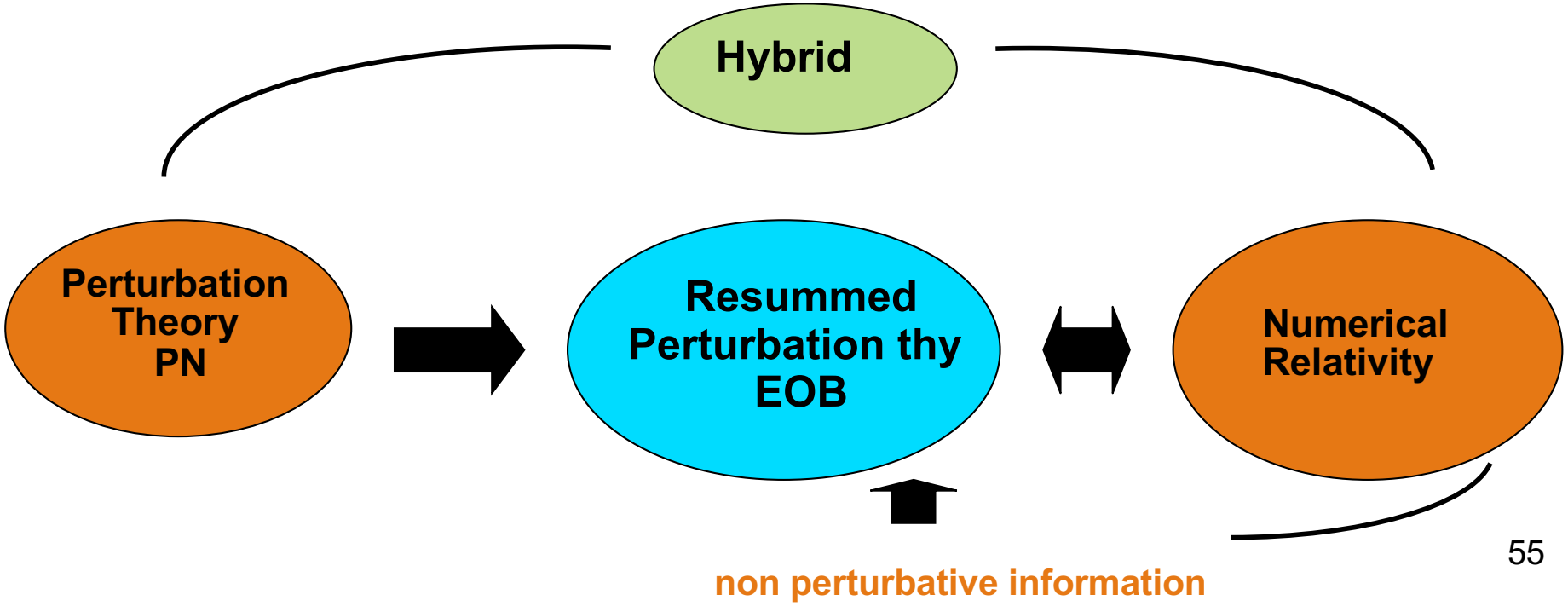

An improved analytical approach

EFFECTIVE ONE BODY (EOB)

approach to the two-body problem

Buonanno,Damour 99	(2 PN Hamiltonian)
Buonanno,Damour 00	(Rad.Reac. full waveform)
Damour, Jaranowski,Schäfer 00	(3 PN Hamiltonian)
Damour 01, Buonanno, Chen, Damour 05,…	(spin)
Damour, Nagar 07, Damour, Iyer, Nagar 08	(factorized waveform)
Buonanno, Cook, Pretorius 07, Buonanno, Pan …	(comparison to NR)
Damour, Nagar 10	(tidal effects)

Binary black hole coalescence: Analytical Relativity

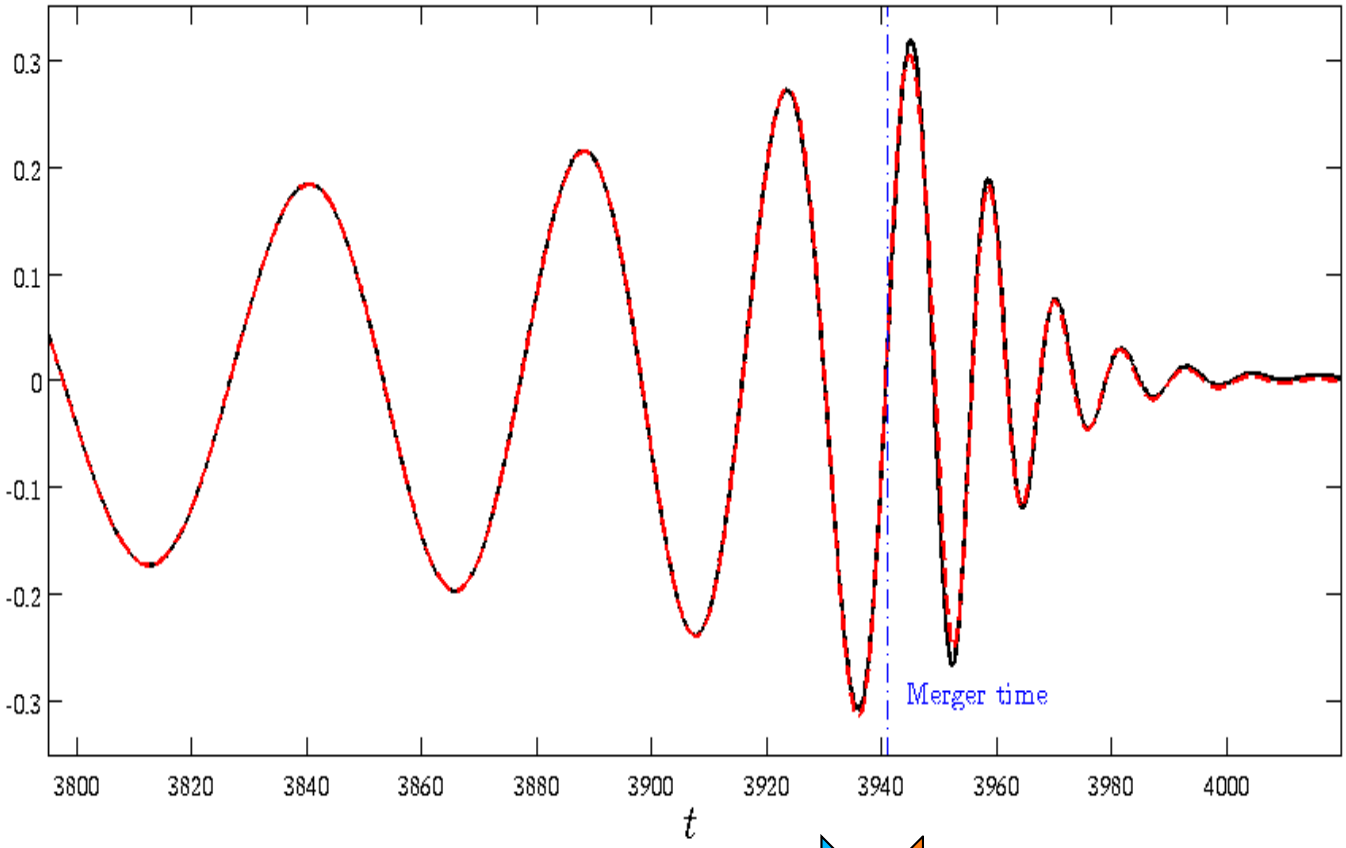

Inspiral + « plunge »

Ringdown

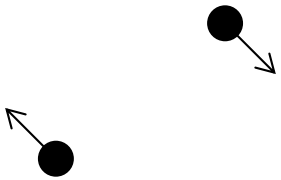

Two orbiting point-masses:
Resummed dynamics

Ringing BH

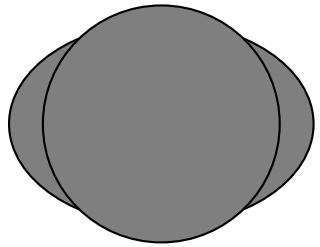

Motion of two point masses

$$S = \int d^D x \frac{R(g)}{16\pi G} - \sum_A \int m_A \sqrt{-g_{\mu\nu}(y_A) dy_A^\mu \, dy_A^\nu}$$

Dimensional continuation : $D = 4 + \varepsilon \ , \ \varepsilon \in \mathbb{C}$

Dynamics : up to 3 loops, i.e. 3 PN

Jaranowski, Schäfer 98
Blanchet, Faye 01
Damour, Jaranowski Schäfer 01
Itoh, Futamase 03
Blanchet, Damour, Esposito-Farèse 04
Foffa, Sturani 11
4PN & 5PN log terms (Damour 10, Blanchet et al 11)
4PN (Jaranowski&Schaefer 13,
Foffa&Sturani 13, Bini&Damour 13)

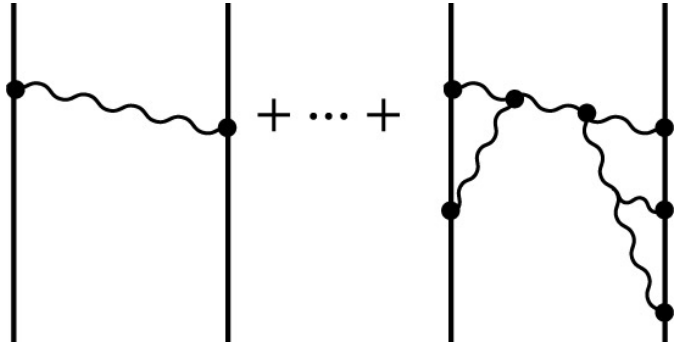

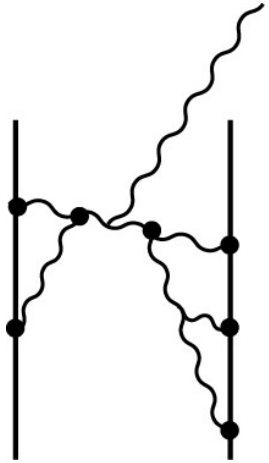

Radiation : up to 3 PN

Blanchet, Iyer, Joguet, 02,
Blanchet, Damour, Esposito-Farèse, Iyer 04
Blanchet, Faye, Iyer, Sinha 08

2-body Taylor-expanded 3PN Hamiltonian [JS98, DJS00,01]

$$H_{\rm N}(\mathbf{x}_a,\mathbf{p}_a)=\sum_a \frac{\mathbf{p}_a^2}{2\,m_a}-\frac{1}{2}\sum_a\sum_{b\neq a}\frac{G\,m_a\,m_b}{r_{ab}}\,.$$

$$H_{\rm 1PN}(\mathbf{x}_a,\mathbf{p}_a)=-\frac{1}{8}\frac{(\mathbf{p}_1^2)^2}{m_1^3}+\frac{1}{8}\frac{Gm_1m_2}{r_{12}}\left[-12\,\frac{\mathbf{p}_1^2}{m_1^2}+14\,\frac{(\mathbf{p}_1\cdot\mathbf{p}_2)}{m_1m_2}+2\,\frac{(\mathbf{n}_{12}\cdot\mathbf{p}_1)(\mathbf{n}_{12}\cdot\mathbf{p}_2)}{m_1m_2}\right]+\frac{1}{4}\frac{Gm_1m_2}{r_{12}}\frac{G(m_1+m_2)}{r_{12}}+(1\longleftrightarrow 2),$$

1PN

$$\begin{aligned}H_{\rm 2PN}(\mathbf{x}_a,\mathbf{p}_a)=&\frac{1}{16}\frac{(\mathbf{p}_1^2)^3}{m_1^5}+\frac{1}{8}\frac{Gm_1m_2}{r_{12}}\left[5\,\frac{(\mathbf{p}_1^2)^2}{m_1^4}-\frac{11}{2}\frac{\mathbf{p}_1^2\,\mathbf{p}_2^2}{m_1^2m_2^2}-\frac{(\mathbf{p}_1\cdot\mathbf{p}_2)^2}{m_1^2m_2^2}+5\,\frac{\mathbf{p}_1^2\,(\mathbf{n}_{12}\cdot\mathbf{p}_2)^2}{m_1^2m_2^2}\right.\\&\left.-6\,\frac{(\mathbf{p}_1\cdot\mathbf{p}_2)\,(\mathbf{n}_{12}\cdot\mathbf{p}_1)(\mathbf{n}_{12}\cdot\mathbf{p}_2)}{m_1^2m_2^2}-\frac{3}{2}\frac{(\mathbf{n}_{12}\cdot\mathbf{p}_1)^2(\mathbf{n}_{12}\cdot\mathbf{p}_2)^2}{m_1^2m_2^2}\right]\\&+\frac{1}{4}\frac{G^2m_1m_2}{r_{12}^2}\left[m_2\left(10\frac{\mathbf{p}_1^2}{m_1^2}+19\frac{\mathbf{p}_2^2}{m_2^2}\right)-\frac{1}{2}(m_1+m_2)\frac{27\,(\mathbf{p}_1\cdot\mathbf{p}_2)+6\,(\mathbf{n}_{12}\cdot\mathbf{p}_1)(\mathbf{n}_{12}\cdot\mathbf{p}_2)}{m_1m_2}\right]\\&-\frac{1}{8}\frac{Gm_1m_2}{r_{12}}\frac{G^2(m_1^2+5m_1m_2+m_2^2)}{r_{12}^2}+(1\longleftrightarrow 2).\end{aligned}$$

2PN

$$\begin{aligned}H_{\rm 3PN}^{\rm reg}(\mathbf{x}_a,\mathbf{p}_a)=&-\frac{5}{128}\frac{(\mathbf{p}_1^2)^4}{m_1^7}+\frac{1}{32}\frac{Gm_1m_2}{r_{12}}\left[-14\,\frac{(\mathbf{p}_1^2)^3}{m_1^6}+4\,\frac{\big((\mathbf{p}_1\cdot\mathbf{p}_2)^2+4\,\mathbf{p}_1^2\,\mathbf{p}_2^2\big)\mathbf{p}_1^2}{m_1^4m_2^2}+\frac{\big(\mathbf{p}_1^2\,\mathbf{p}_2^2-2\,(\mathbf{p}_1\cdot\mathbf{p}_2)^2\big)(\mathbf{p}_1\cdot\mathbf{p}_2)}{m_1^3m_2^3}\right.\\&-10\,\frac{\big(\mathbf{p}_1^2\,(\mathbf{n}_{12}\cdot\mathbf{p}_2)^2+\mathbf{p}_2^2\,(\mathbf{n}_{12}\cdot\mathbf{p}_1)^2\big)\mathbf{p}_1^2}{m_1^4m_2^2}+24\,\frac{\mathbf{p}_1^2\,(\mathbf{p}_1\cdot\mathbf{p}_2)(\mathbf{n}_{12}\cdot\mathbf{p}_1)(\mathbf{n}_{12}\cdot\mathbf{p}_2)}{m_1^4m_2^2}+2\,\frac{\mathbf{p}_1^2\,(\mathbf{p}_1\cdot\mathbf{p}_2)(\mathbf{n}_{12}\cdot\mathbf{p}_2)^2}{m_1^3m_2^3}\\&+\frac{\big(7\,\mathbf{p}_1^2\,\mathbf{p}_2^2-10\,(\mathbf{p}_1\cdot\mathbf{p}_2)^2\big)(\mathbf{n}_{12}\cdot\mathbf{p}_1)(\mathbf{n}_{12}\cdot\mathbf{p}_2)}{m_1^3m_2^3}+6\,\frac{\mathbf{p}_1^2\,(\mathbf{n}_{12}\cdot\mathbf{p}_1)^2(\mathbf{n}_{12}\cdot\mathbf{p}_2)^2}{m_1^4m_2^2}\\&\left.+15\,\frac{(\mathbf{p}_1\cdot\mathbf{p}_2)(\mathbf{n}_{12}\cdot\mathbf{p}_1)^2(\mathbf{n}_{12}\cdot\mathbf{p}_2)^2}{m_1^3m_2^3}-18\,\frac{\mathbf{p}_1^2\,(\mathbf{n}_{12}\cdot\mathbf{p}_1)(\mathbf{n}_{12}\cdot\mathbf{p}_2)^3}{m_1^3m_2^3}+5\,\frac{(\mathbf{n}_{12}\cdot\mathbf{p}_1)^3(\mathbf{n}_{12}\cdot\mathbf{p}_2)^3}{m_1^3m_2^3}\right]\\&+\frac{G^2m_1m_2}{r_{12}^2}\left[\frac{1}{16}(m_1-27m_2)\frac{(\mathbf{p}_1^2)^2}{m_1^4}-\frac{115}{16}m_1\frac{\mathbf{p}_1^2\,(\mathbf{p}_1\cdot\mathbf{p}_2)}{m_1^3m_2}+\frac{1}{48}m_2\frac{25\,(\mathbf{p}_1\cdot\mathbf{p}_2)^2+371\,\mathbf{p}_1^2\,\mathbf{p}_2^2}{m_1^2m_2^2}\right.\\&+\frac{17}{16}\frac{\mathbf{p}_1^2(\mathbf{n}_{12}\cdot\mathbf{p}_1)^2}{m_1^3}-\frac{1}{8}m_1\frac{\big(15\,\mathbf{p}_1^2\,(\mathbf{n}_{12}\cdot\mathbf{p}_2)+11\,(\mathbf{p}_1\cdot\mathbf{p}_2)\,(\mathbf{n}_{12}\cdot\mathbf{p}_1)\big)(\mathbf{n}_{12}\cdot\mathbf{p}_1)}{m_1^3m_2}+\frac{5}{12}\frac{(\mathbf{n}_{12}\cdot\mathbf{p}_1)^4}{m_1^3}\\&-\frac{3}{2}m_1\frac{(\mathbf{n}_{12}\cdot\mathbf{p}_1)^3(\mathbf{n}_{12}\cdot\mathbf{p}_2)}{m_1^3m_2}+\frac{125}{12}m_2\frac{(\mathbf{p}_1\cdot\mathbf{p}_2)\,(\mathbf{n}_{12}\cdot\mathbf{p}_1)(\mathbf{n}_{12}\cdot\mathbf{p}_2)}{m_1^2m_2^2}+\frac{10}{3}m_2\frac{(\mathbf{n}_{12}\cdot\mathbf{p}_1)^2(\mathbf{n}_{12}\cdot\mathbf{p}_2)^2}{m_1^2m_2^2}\\&\left.-\frac{1}{48}(220m_1+193m_2)\frac{\mathbf{p}_1^2(\mathbf{n}_{12}\cdot\mathbf{p}_2)^2}{m_1^2m_2^2}\right]+\frac{G^3m_1m_2}{r_{12}^3}\left[-\frac{1}{48}\left(466\,m_1^2+\left(473-\frac{3}{4}\pi^2\right)m_1m_2+150\,m_2^2\right)\frac{\mathbf{p}_1^2}{m_1^2}\right.\\&+\frac{1}{16}\left(77(m_1^2+m_2^2)+\left(143-\frac{1}{4}\pi^2\right)m_1m_2\right)\frac{(\mathbf{p}_1\cdot\mathbf{p}_2)}{m_1m_2}+\frac{1}{16}\left(61\,m_1^2-\left(43+\frac{3}{4}\pi^2\right)m_1m_2\right)\frac{(\mathbf{n}_{12}\cdot\mathbf{p}_1)^2}{m_1^2}\\&\left.+\frac{1}{16}\left(21(m_1^2+m_2^2)+\left(119+\frac{3}{4}\pi^2\right)m_1m_2\right)\frac{(\mathbf{n}_{12}\cdot\mathbf{p}_1)(\mathbf{n}_{12}\cdot\mathbf{p}_2)}{m_1m_2}\right]\\&+\frac{1}{8}\frac{G^4m_1m_2^3}{r_{12}^4}\left[\left(\frac{227}{3}-\frac{21}{4}\pi^2\right)m_1+m_2\right]+(1\longleftrightarrow 2).\end{aligned}\qquad(12)$$

3PN

Taylor-expanded 3PN waveform

Blanchet,Iyer, Joguet 02, Blanchet, Damour, Esposito-Farese, Iyer 04, Kidder 07, Blanchet et al. 08

$$h^{22} = -8\sqrt{\frac{\pi}{5}}\frac{G\nu m}{c^2 R}e^{-2i\phi}x\Big\{1 - x\Big(\frac{107}{42} - \frac{55}{42}\nu\Big) + x^{3/2}\Big[2\pi + 6i\ln\Big(\frac{x}{x_0}\Big)\Big] - x^2\Big(\frac{2173}{1512} + \frac{1069}{216}\nu - \frac{2047}{1512}\nu^2\Big)$$
$$- x^{5/2}\Big[\Big(\frac{107}{21} - \frac{34}{21}\nu\Big)\pi + 24i\nu + \Big(\frac{107i}{7} - \frac{34i}{7}\nu\Big)\ln\Big(\frac{x}{x_0}\Big)\Big]$$
$$+ x^3\Big[\frac{27\,027\,409}{646\,800} - \frac{856}{105}\gamma_E + \frac{2}{3}\pi^2 - \frac{1712}{105}\ln 2 - \frac{428}{105}\ln x$$
$$- 18\Big[\ln\Big(\frac{x}{x_0}\Big)\Big]^2 - \Big(\frac{278\,185}{33\,264} - \frac{41}{96}\pi^2\Big)\nu - \frac{20\,261}{2772}\nu^2 + \frac{114\,635}{99\,792}\nu^3 + \frac{428i}{105}\pi + 12i\pi\ln\Big(\frac{x}{x_0}\Big)\Big] + O(\epsilon^{7/2})\Big\},$$

$$x = (M\Omega)^{2/3} \sim v^2/c^2$$

$$M = m_1 + m_2$$
$$\nu = m_1 m_2/(m_1 + m_2)^2$$

Simple way to estimate frequency at merger:
Last stable circular orbit around a black hole

$$r_{\mathrm{LSCO}} = 6\,\frac{G\,(m_1+m_2)}{c^2}$$

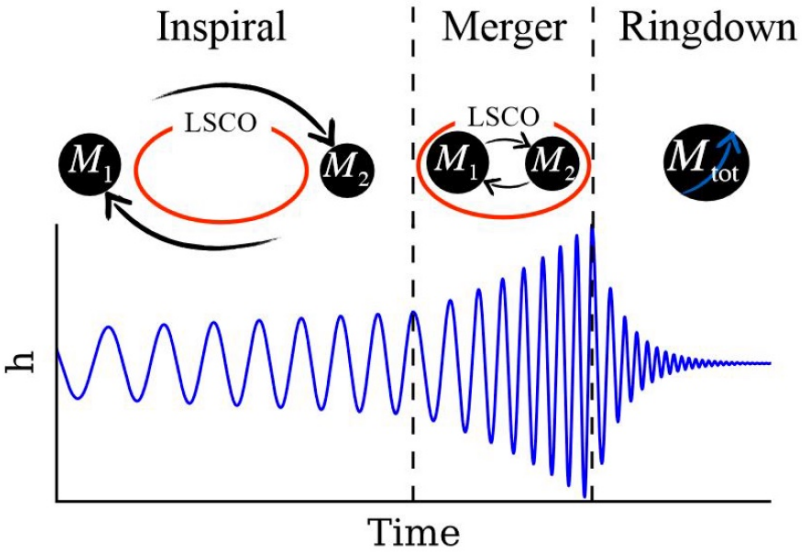

$$\omega_{\mathrm{GW,LSCO}} = 2\sqrt{\frac{G\,(m_1+m_2)}{r_{\mathrm{LSCO}}^3}} = \frac{2\,c^3}{6^{3/2}\,G\,(m_1+m_2)}$$

$$\boxed{\omega_{\mathrm{GW,LSCO}} = 460\,\mathrm{Hz}\,\frac{60\,M_{\mathrm{sun}}}{(m_1+m_2)}}$$

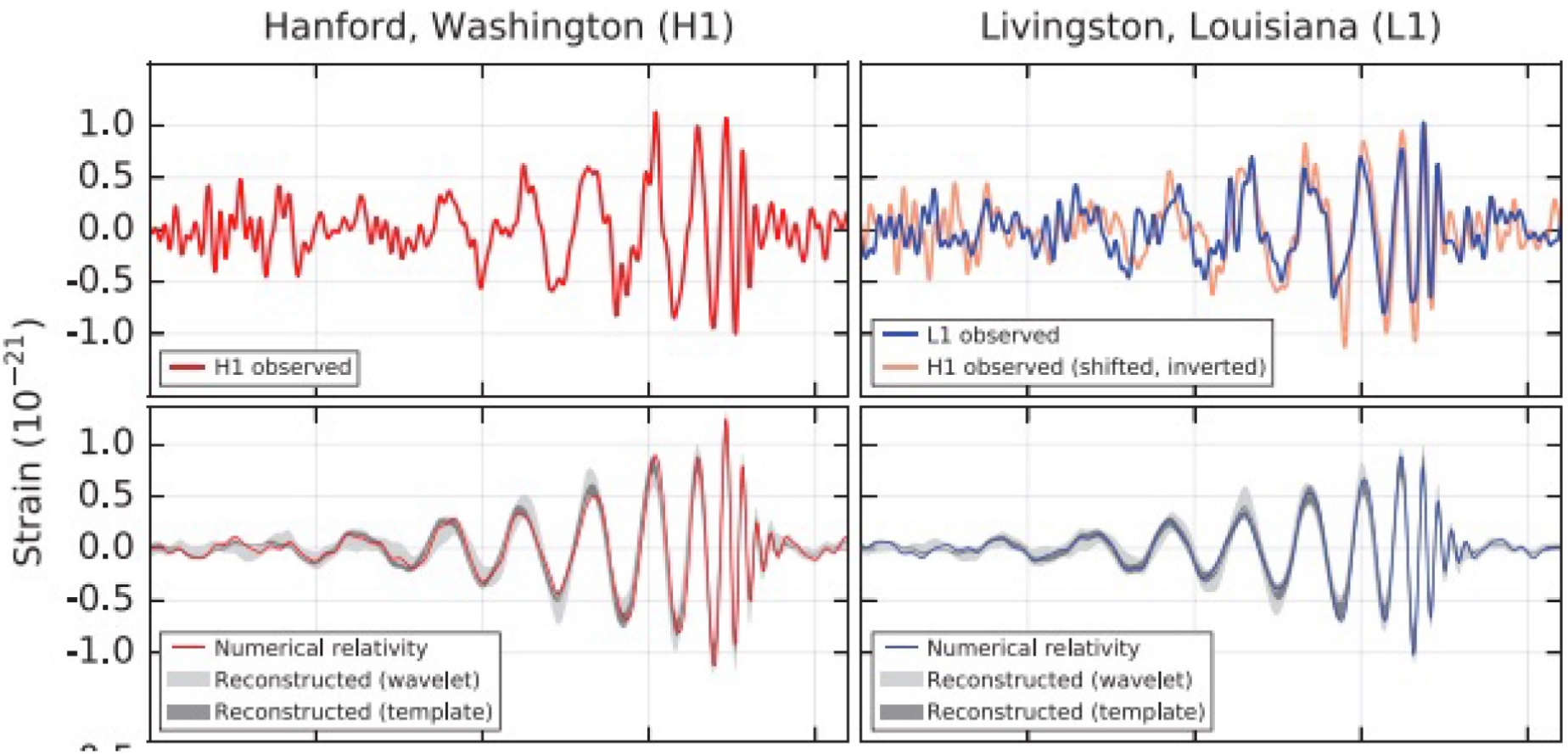

Abbott et al. 2016

Detectors:

Advanced LIGO (Livingstone + Hanford, US)
Advanced Virgo (Pisa, Italy)

Michelson interferometers

Design started in the '90s
First science runs ~ 2007 (no detection)
Being upgraded in 2007 – 2015
First run advanced detectors 2015

Time schedule

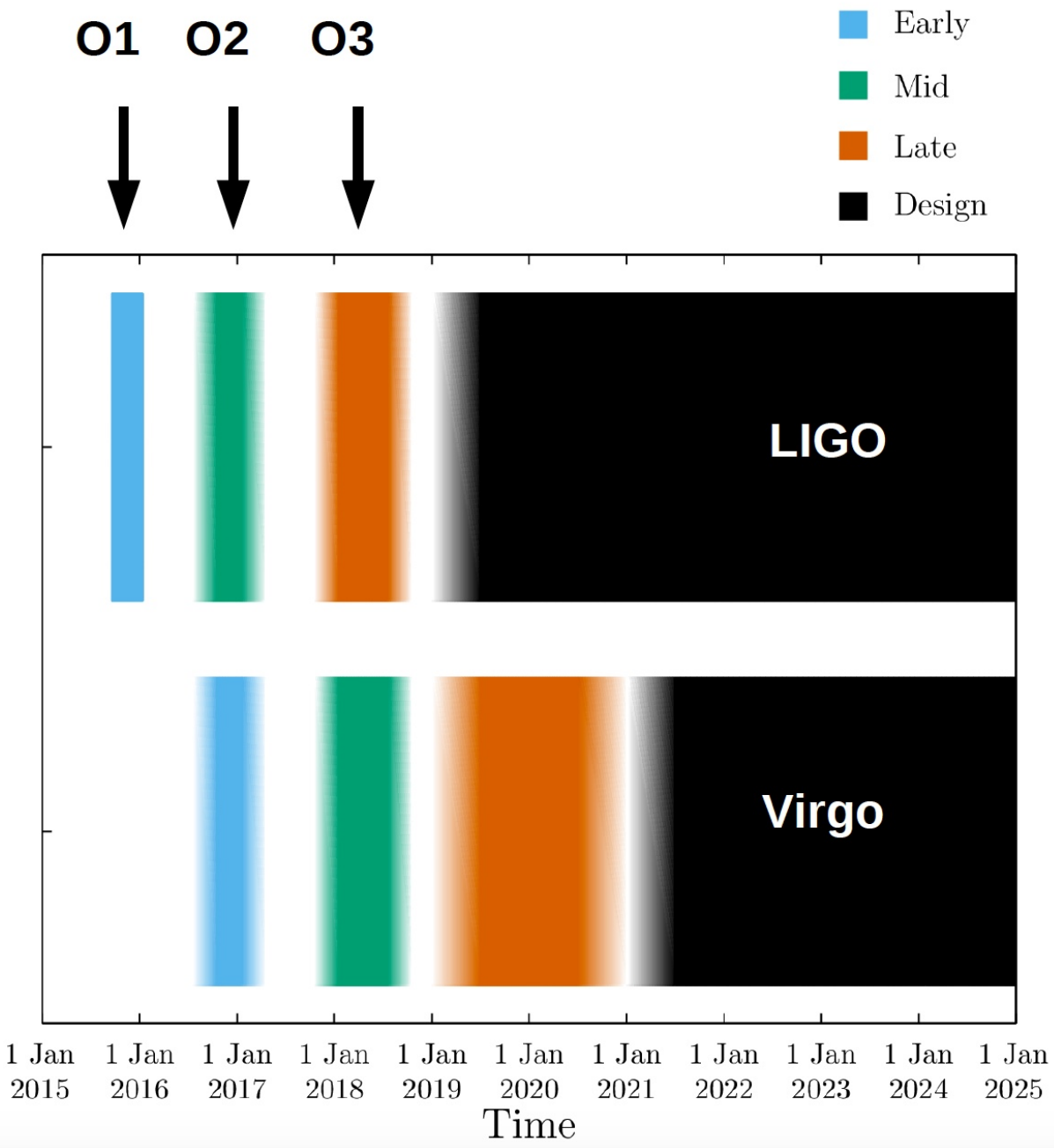

Frequency range: ~ 10 – 10'000 Hz

Suitable for mergers of compact binaries

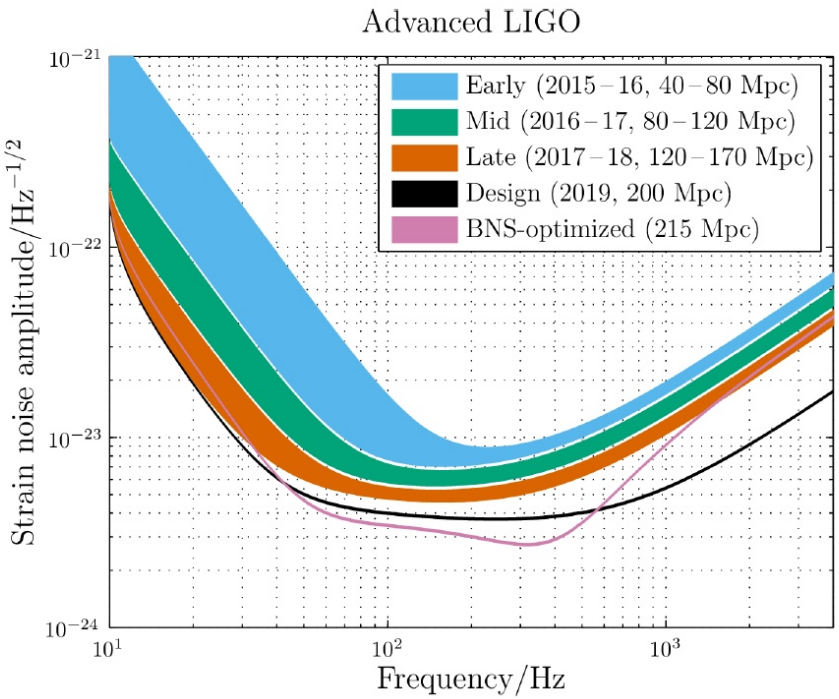

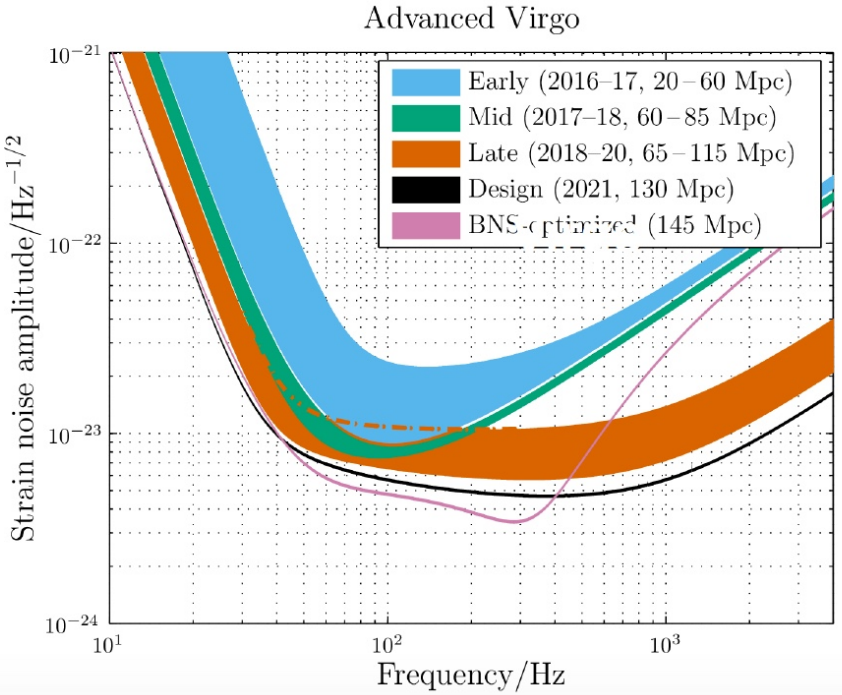

Noise level of LIGO & Virgo
(Noise power spectral density)

Summary of detections:

2015/09/12	first LIGO run	
2015/09/14	GW150914	black holes (BHs)
2015/10/12	LVT151012	maybe BHs
2015/12/26	GW151226	BHs
2015/01 – 2016/11	detectors switched off	
2017/01/04	GW170104	BHs
2017/08/01	Virgo joins LIGO	
2017/08/14	GW170814	BHs
2017/08/17	GW170817	neutron stars (NSs)
2017/08/25 – now	detectors switched off	

Properties of the first detections:

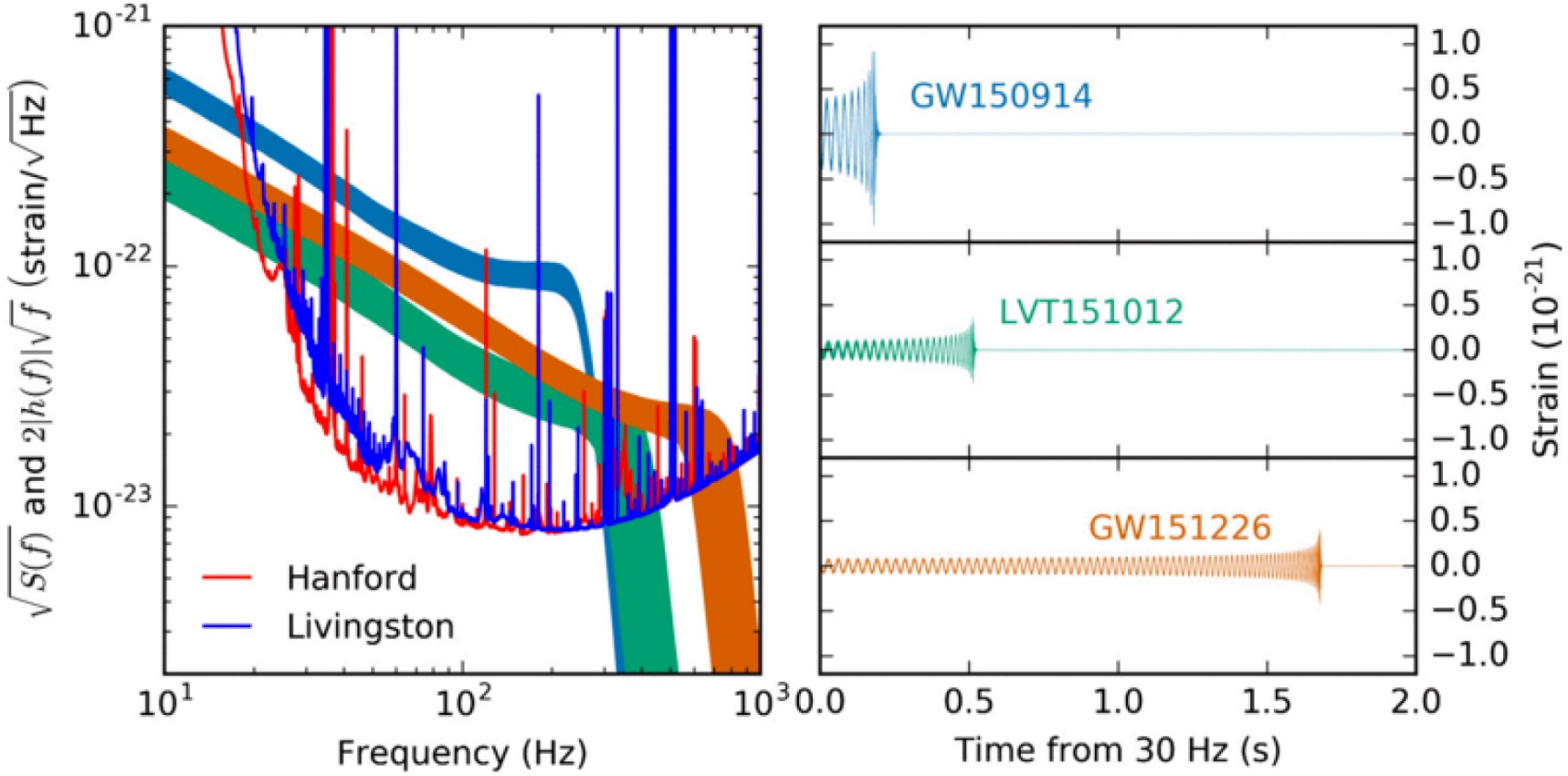

From Abbott et al. (2016)
https://journals.aps.org/prx/abstract/10.1103/PhysRevX.6.041015#fulltext

GW detection

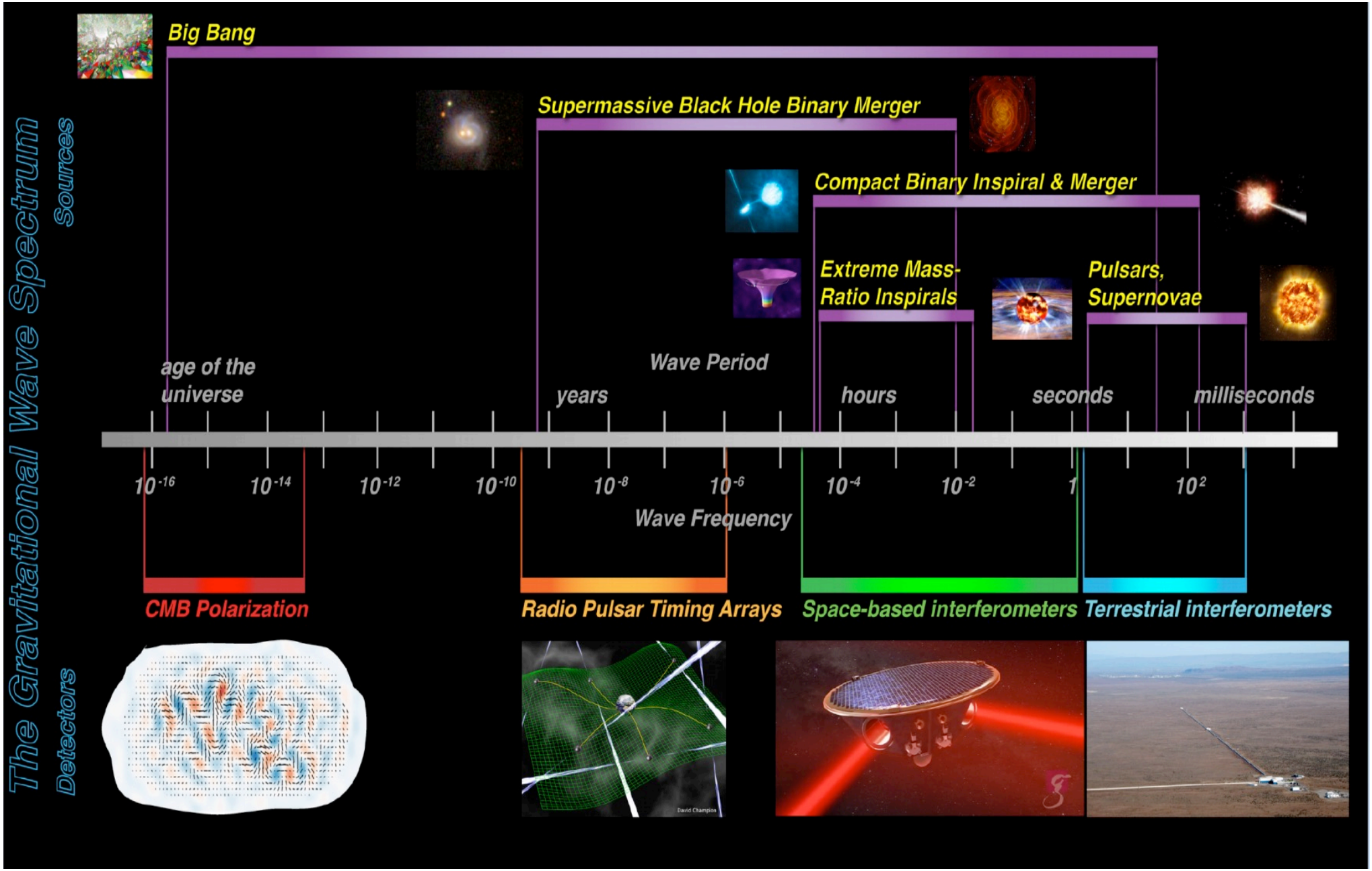

GW detection

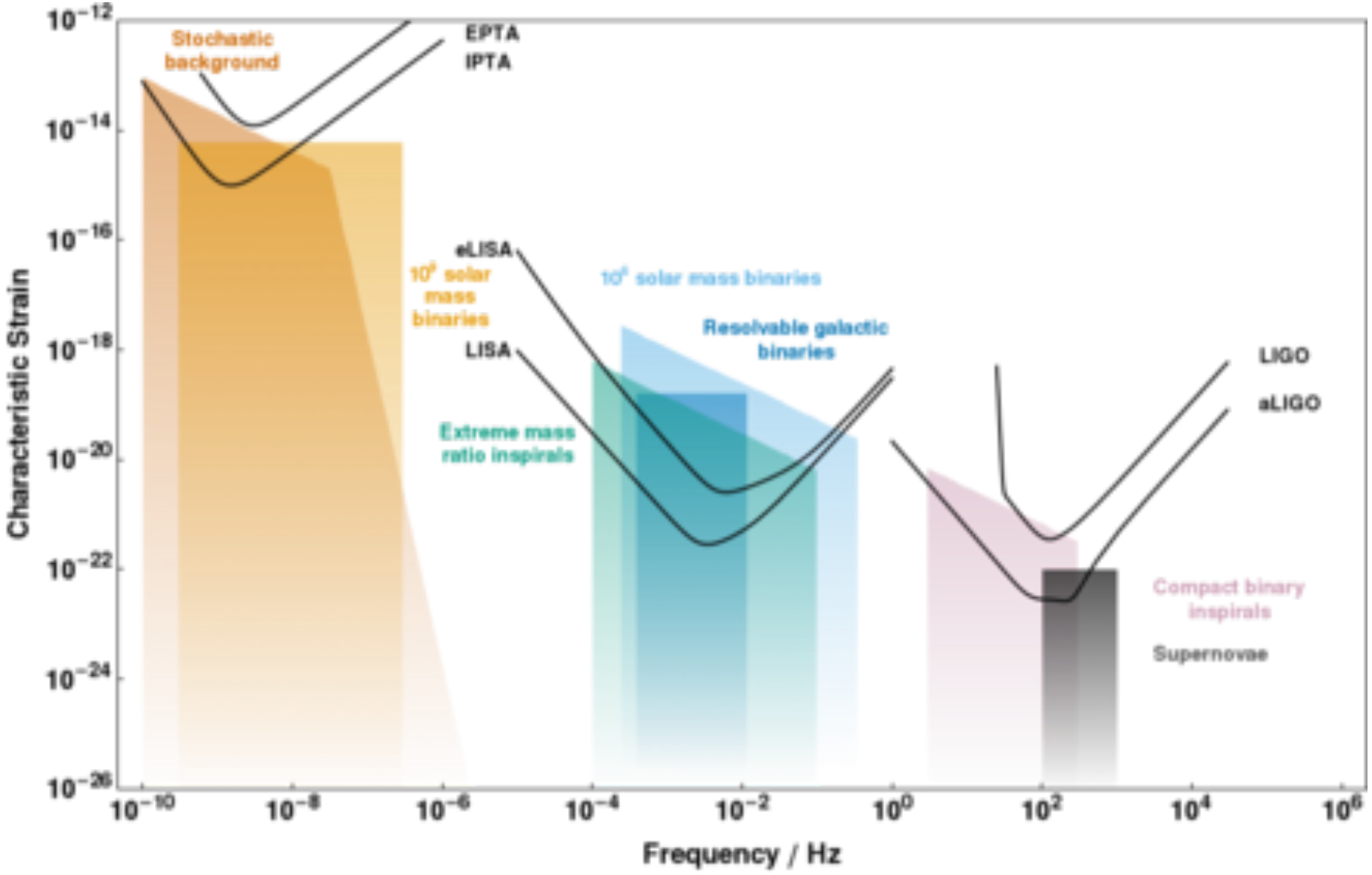

Localization LIGO O1 Events

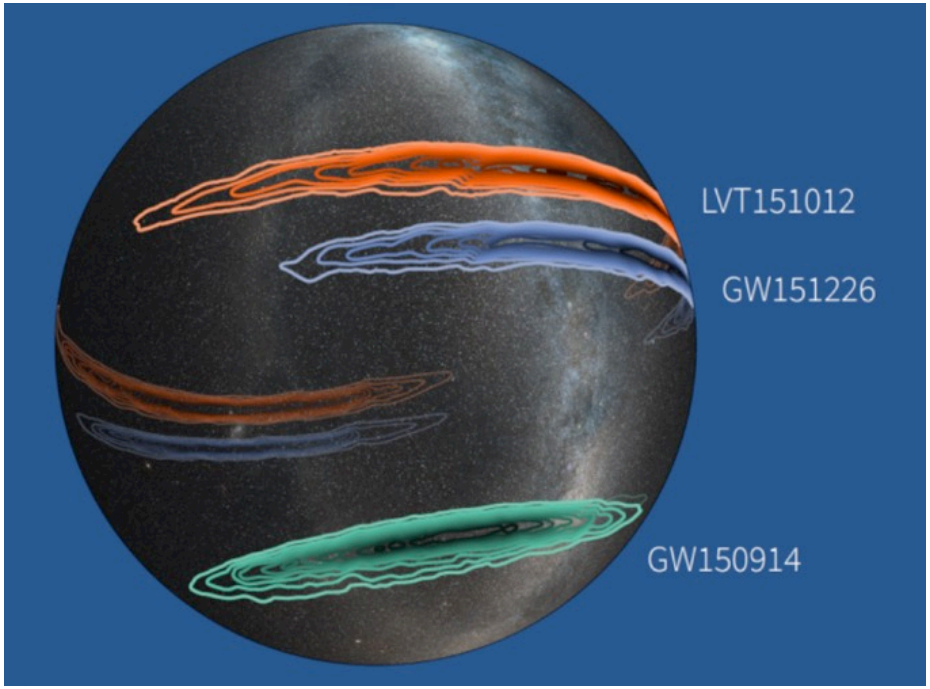

for GW150914: Astrophys. J. Lett. 826, L13 (2016)

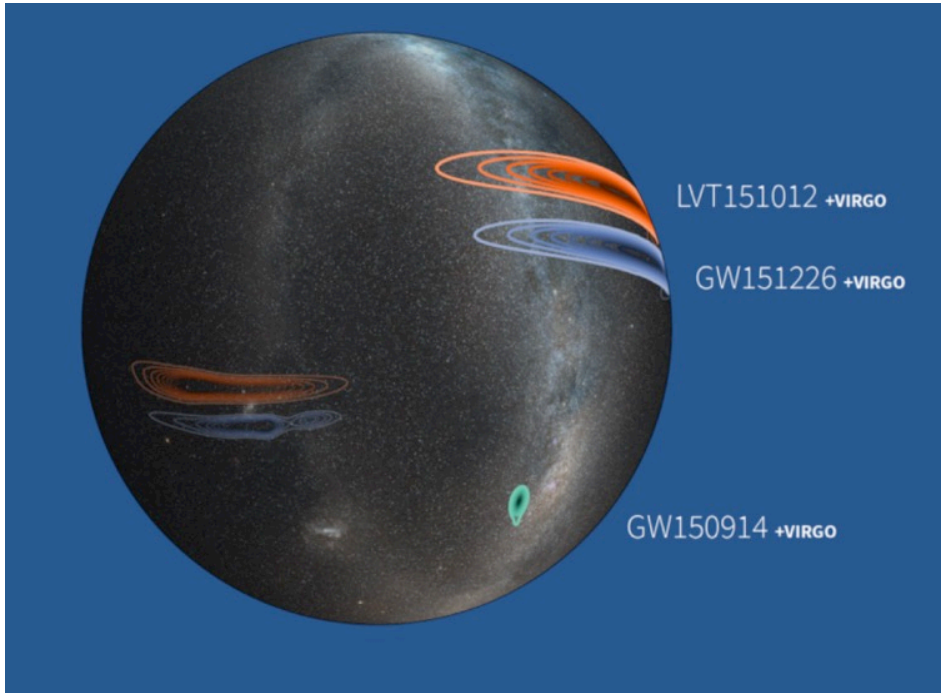

Simulation for 3rd detector at Virgo location with LIGO O1 sensitivity

GW detector network: 2015-2025

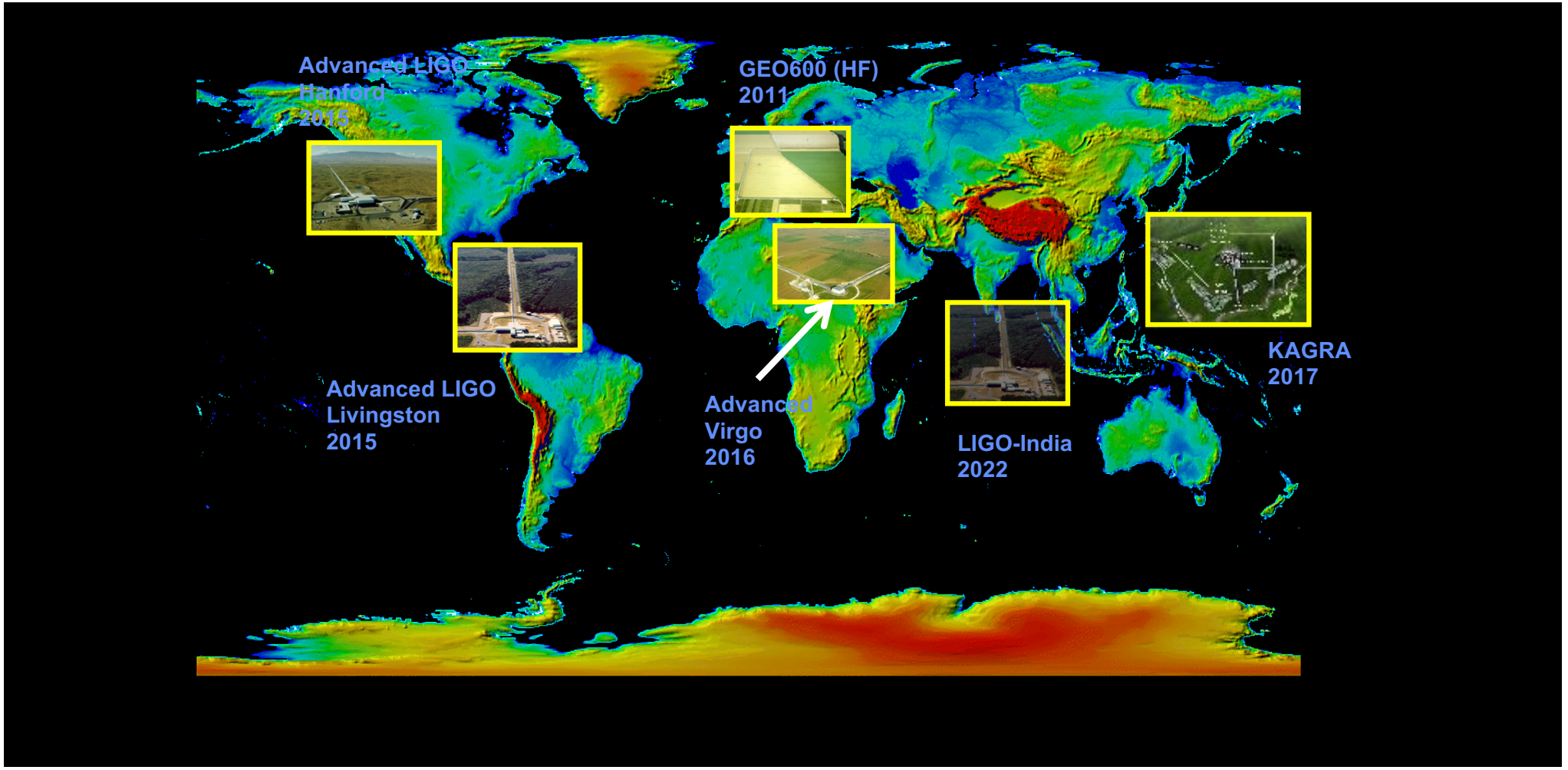

KAGRA

Kamioka Mine

- **Technologies crucial for next-generation detectors;**
- **KAGRA can be regarded as a 2.5-generation detector.**

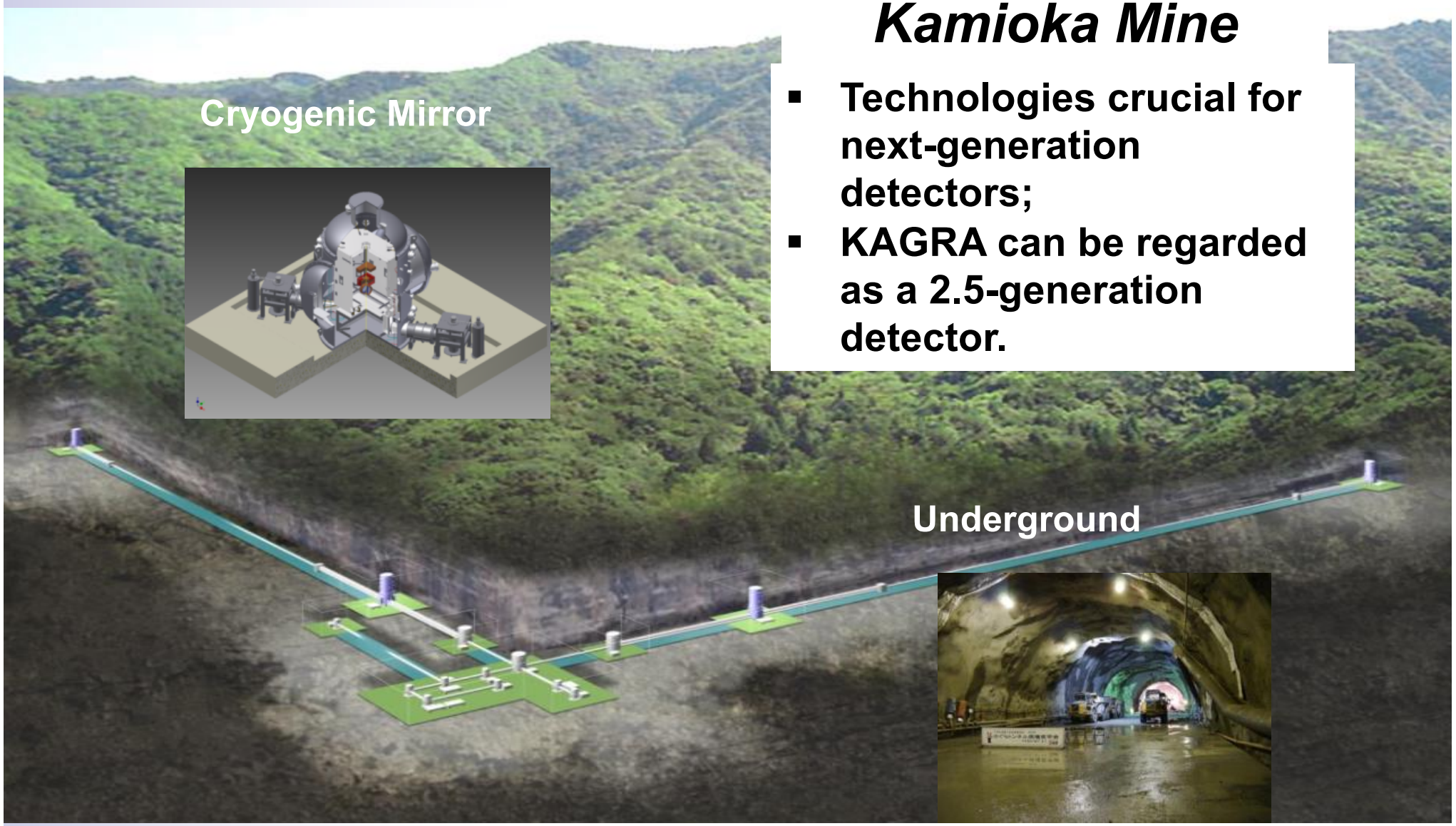

Third Generation Gravitational Wave Detectors

Einstein Telescope

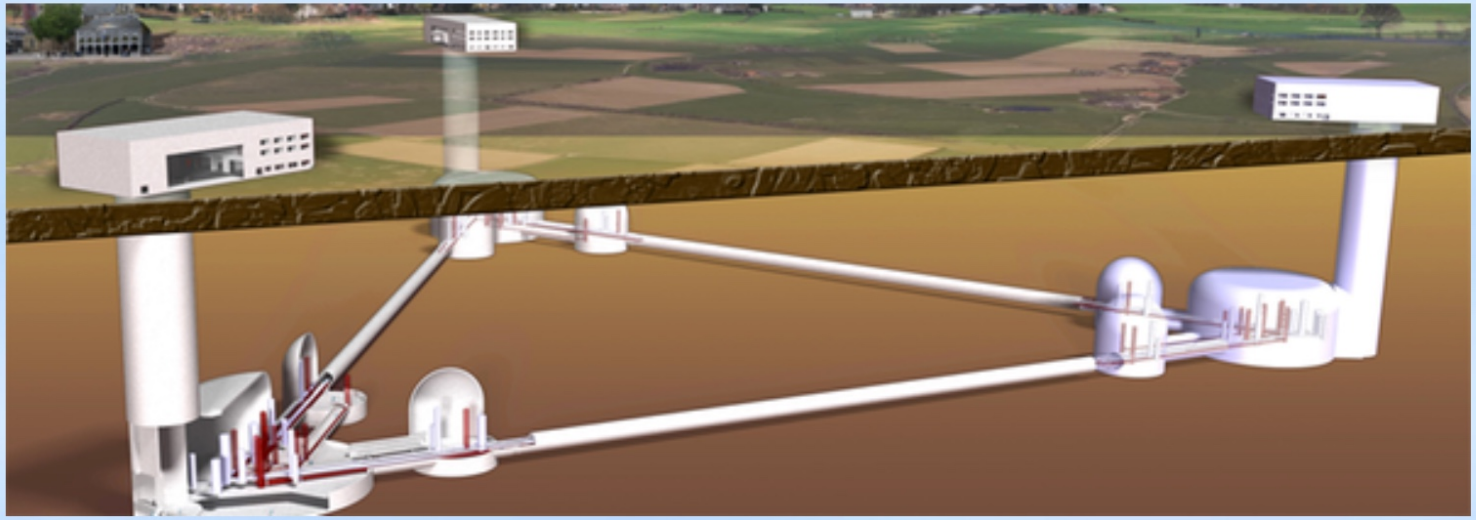

Underground to reduced seismic noise.
10 km arms
Cryogenic mirrors
Lower frequency limit – 1 Hz
10 x better sensitivity than 2nd generation detectors
Farther back in the universe

M. Punturo talk

Cosmic Explorer

Preliminary Concept

The Cosmic Explorer: x10 aLIGO

- Earth‘s Surface;
- 40 km arms
- Advanced LIGO Technology +
- Squeezed Light

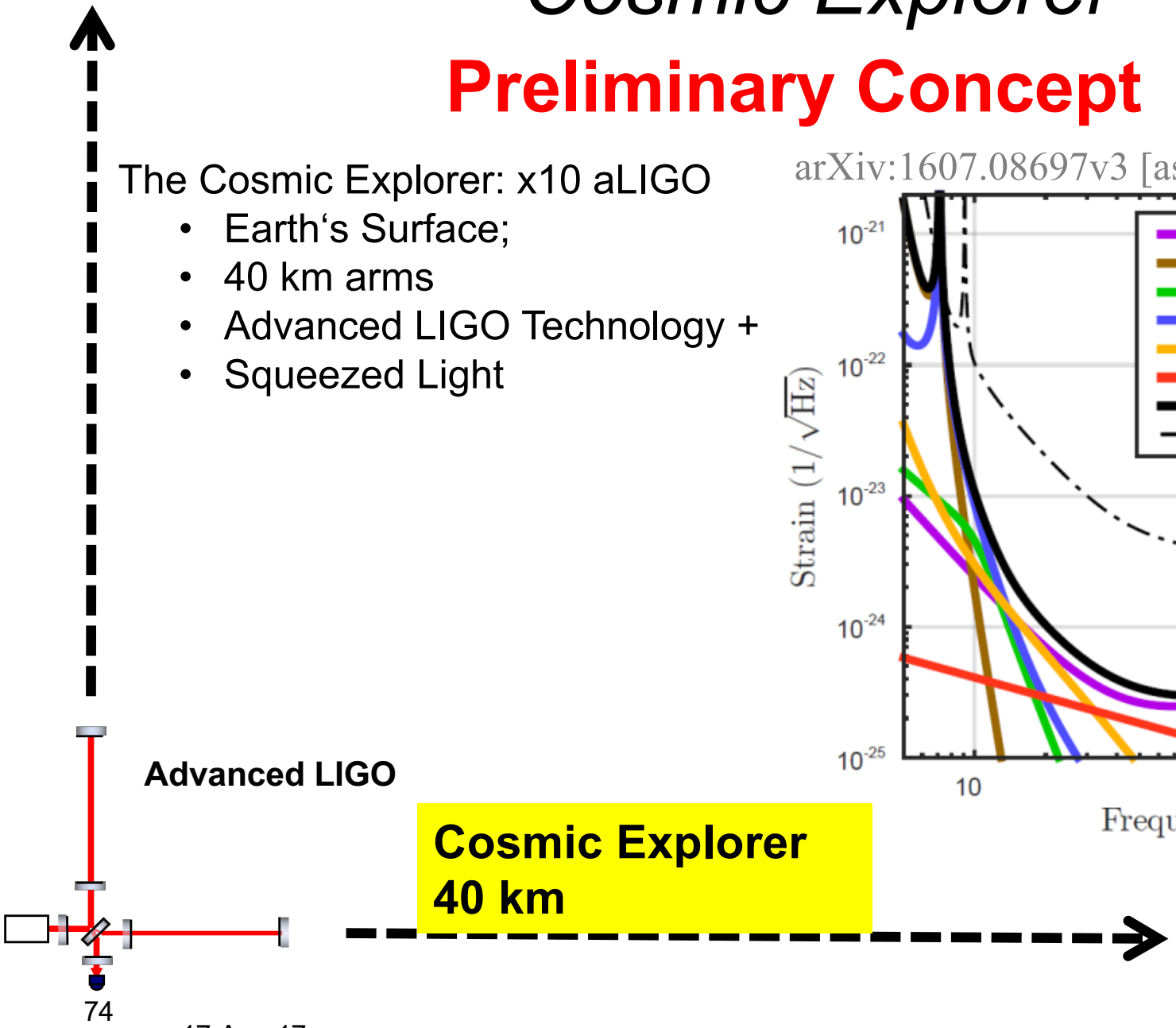

arXiv:1607.08697v3 [astro-ph.IM] 11 Sep 2016

Third Generation Gravitational Wave Detectors

With Einstein Telescope (European) or Cosmic Explorer (US) almost every stellar mass binary black hole merger in the observable universe will be detectable.

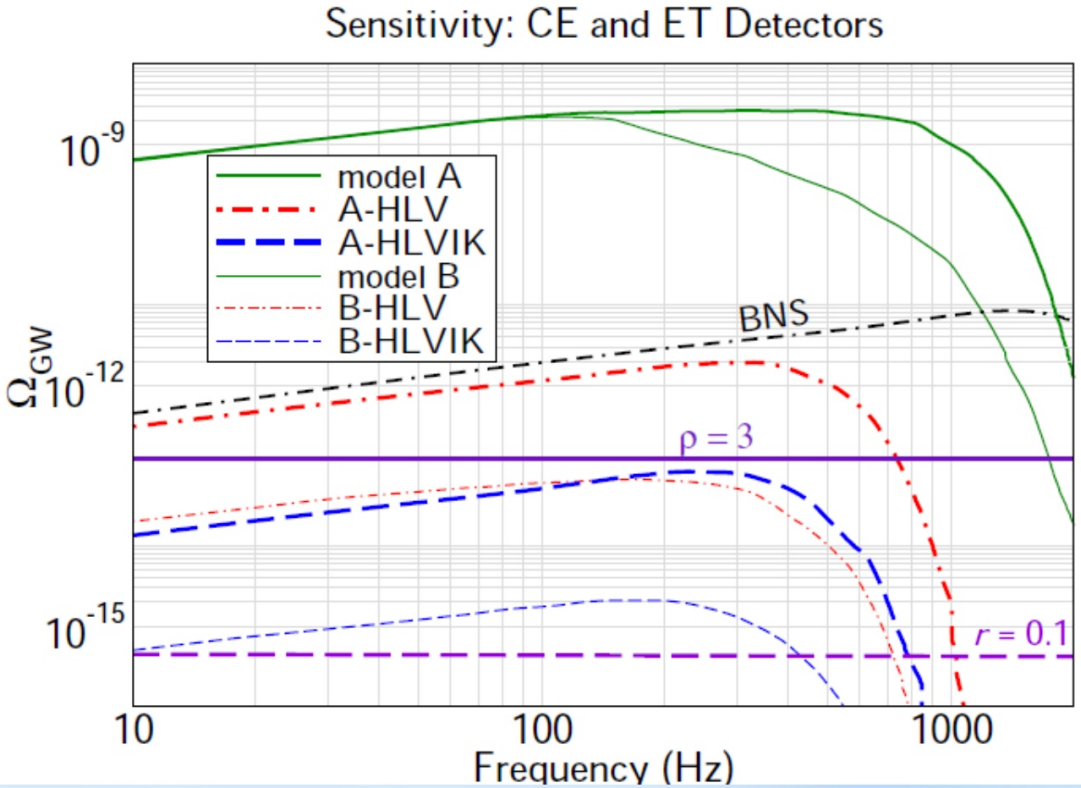

BBH confusion background can potentially be subtracted to observe the primordial background at the level of $\Omega_{GW} \sim 10^{-13}$ after five years of observation.

Arxiv:1611.08943

Space missions

Laser Interferometer Space Antenna - LISA

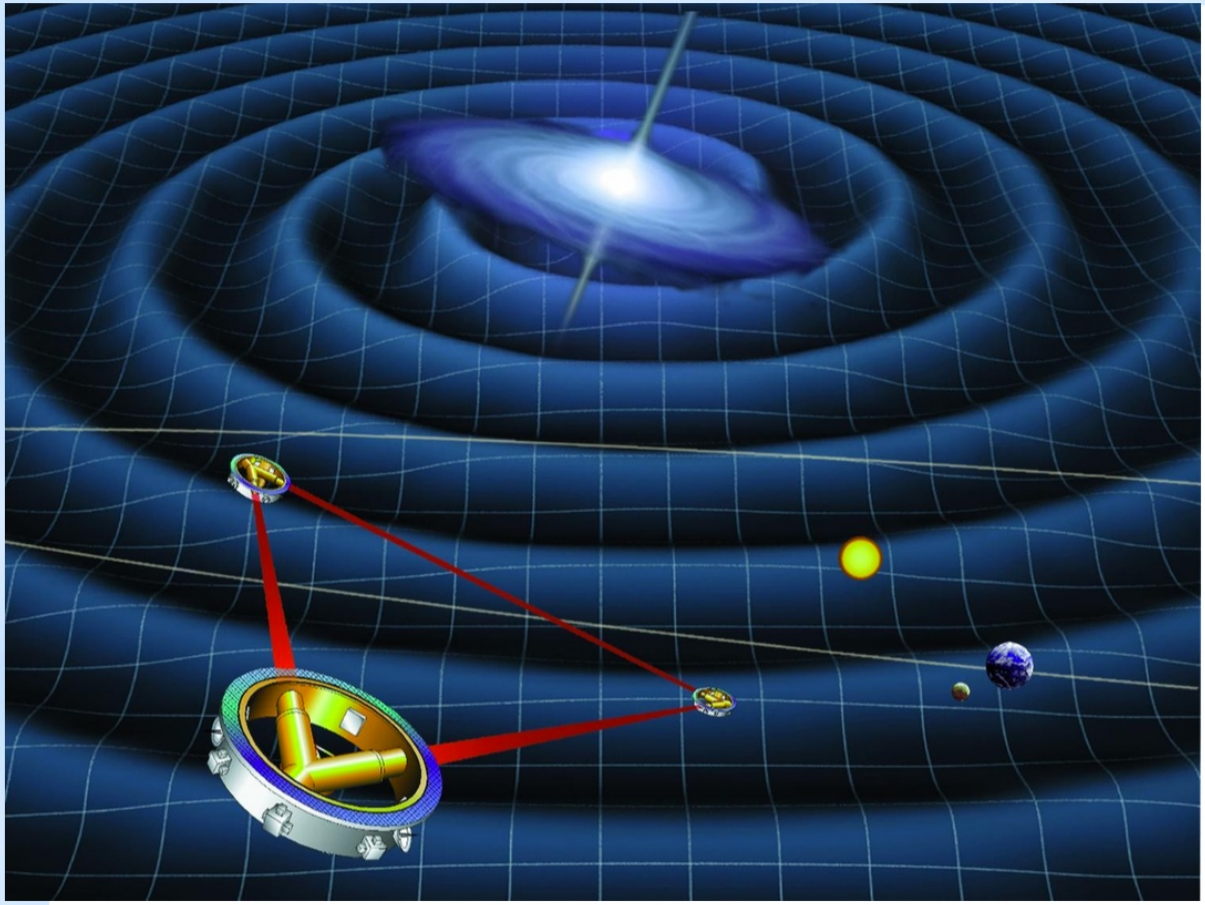

Present plan: 3 Interferometers
2.5×10^6 km arm lengths

ESA – All Systems GO!

Recent “Call” for mission

Acceptance - soon?

Planned launch 2034

NASA coming back

Earlier launch? 2028?

LIGO GW events and Lisa Pathfinder success have helped significantly

Tremendous activity at present

LISA in Orbit

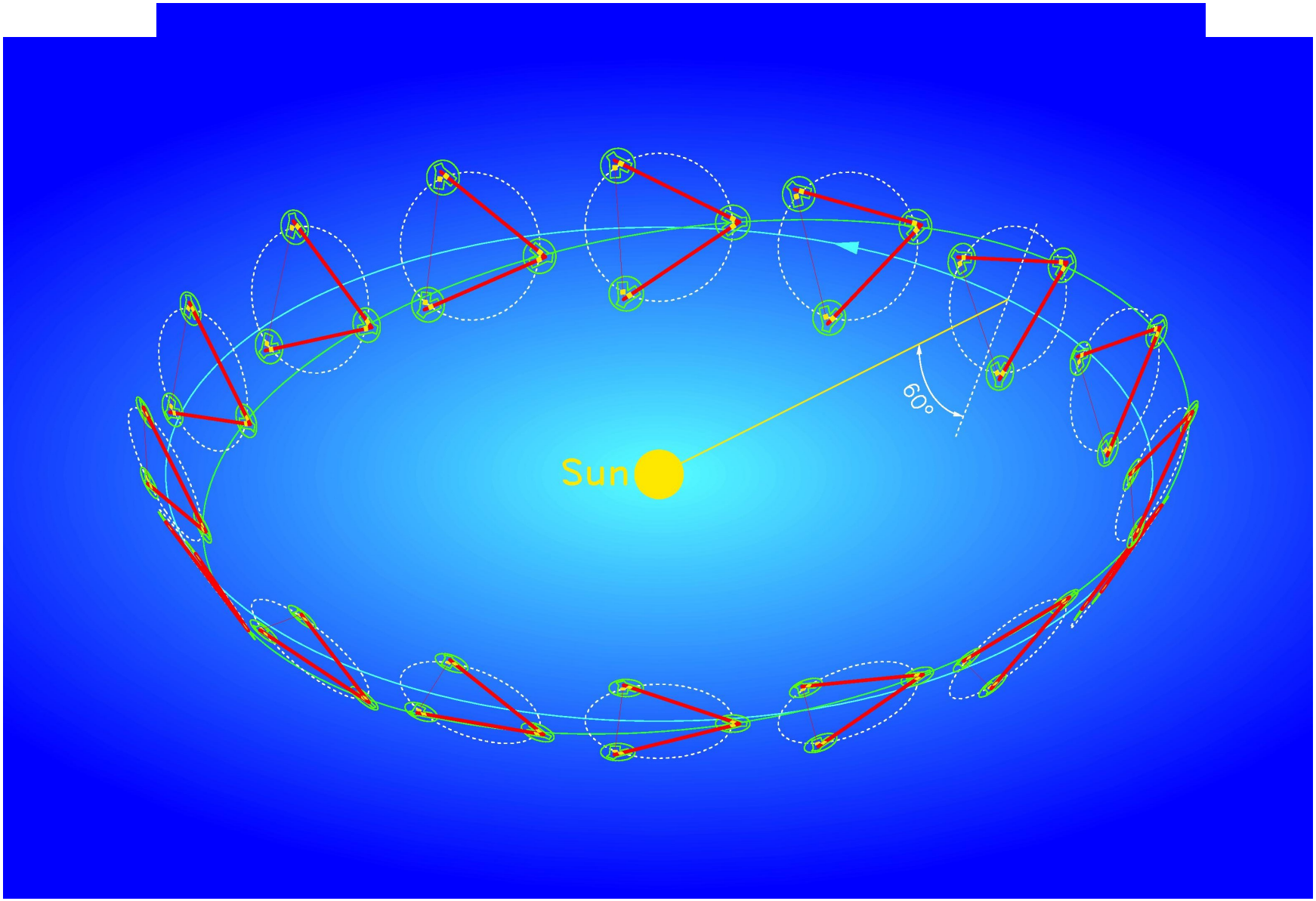

LISA physics

- the nature of gravity
- the fundamental nature of black holes
- black holes as sources of energy
- nonlinear structure formation
- dynamics of galactic nuclei
- formation and evolution of stellar binary systems
- the very early universe
- cosmography (specifically, the cosmic distance scale)

Gravitational Observatory Advisory Team – GOAT (ESA web site)

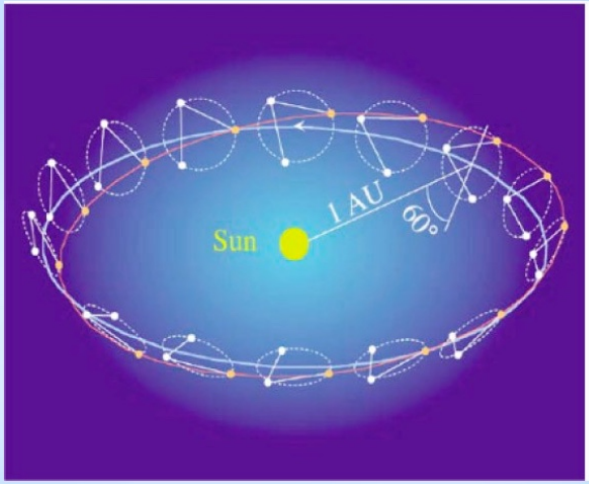

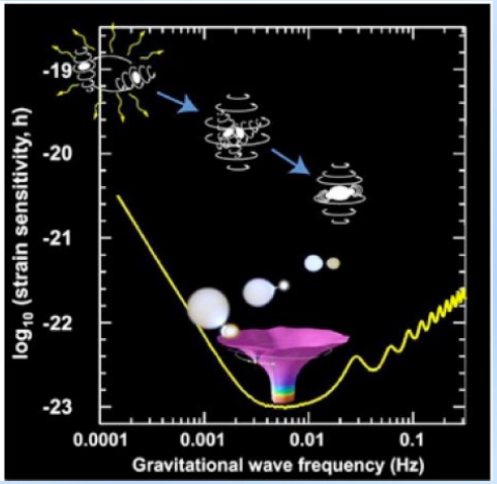

LISA Pathfinder – Demonstrating LISA Technology

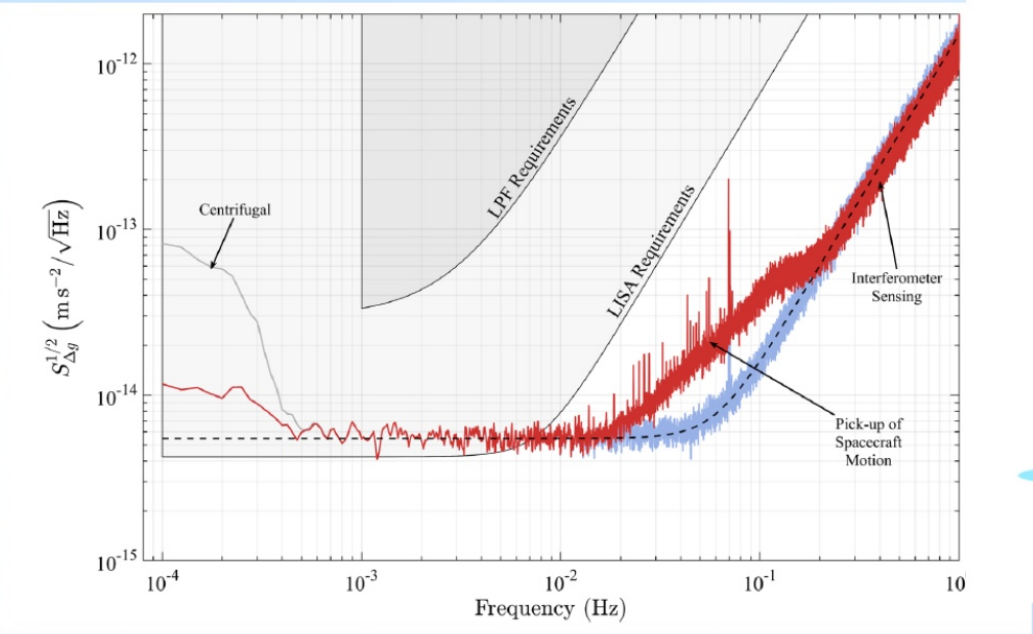

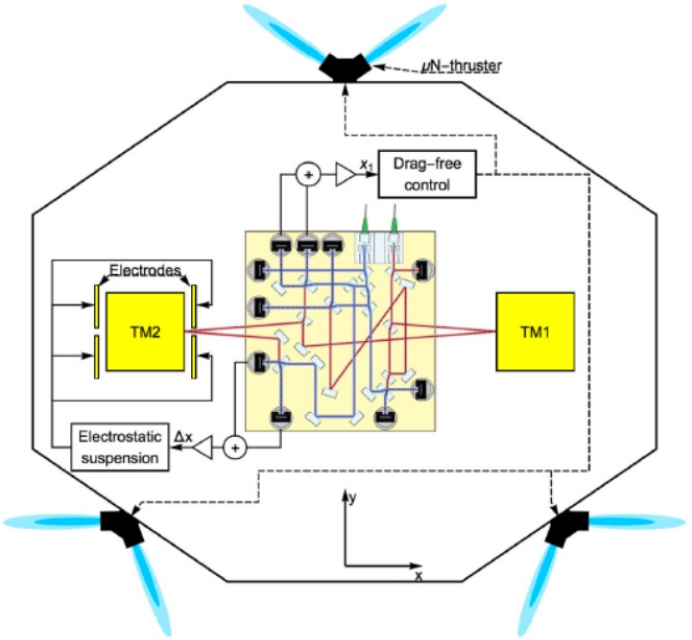

LISA Pathfinder worked! Exceeded requirements. Still, operation was not perfect, and there is lots of experimental work to do before LISA.

A set of cold gas micro-newton thrusters to ensure the spacecraft follows TM1. A second control loop forces TM2 to stay at a fixed distance from TM1 and thus centered in its own electrode housing.

PRL **116**, 231101 (2016)